Biochimica et Biophysica Acta 1837 (2014) 562–577

Contents lists available at ScienceDirect

Biochimica et Biophysica Acta

journal homepage: www.elsevier.com/locate/bbabio

Review

Molecular and evolutionary aspects of microbial sensory rhodopsins ☆

Keiichi Inoue [a,b], Takashi Tsukamoto [c], Yuki Sudo [b,c,d,*]

[a] Department of Frontier Materials, Nagoya Institute of Technology, Showa-ku, Nagoya 466–8555, Japan
[b] Japan Science and Technology Agency (JST), PRESTO, 4-1-8 Honcho Kawaguchi, Saitama 332–0012, Japan
[c] Division of Biological Science, Graduate School of Science, Nagoya University, Nagoya, 464–8602, Japan
[d] Department of Life and Coordination-Complex Molecular Science, Institute for Molecular Science, 38 Nishigo-Naka, Myodaiji, Okazaki, Japan

ARTICLE INFO

Article history:
Received 15 April 2013
Received in revised form 14 May 2013
Accepted 16 May 2013
Available online 1 June 2013

Keywords:
Retinal
Signal transfer
Membrane protein
Phototaxis

ABSTRACT

Retinal proteins (~rhodopsins) are photochemically reactive membrane-embedded proteins, with seven transmembrane α-helices which bind the chromophore retinal (vitamin A aldehyde). They are widely distributed through all three biological kingdoms, eukarya, bacteria and archaea, indicating the biological significance of the retinal proteins. Light absorption by the retinal proteins triggers a photoisomerization of the chromophore, leading to the biological function, light-energy conversion or light-signal transduction. This article reviews molecular and evolutionary aspects of the light-signal transduction by microbial sensory receptors and their related proteins. This article is part of a Special Issue entitled: Retinal Proteins - You can teach an old dog new tricks.

1. Introduction

1.1. Conversion of light energy into an electrochemical potential with microbial rhodopsins

Biological molecules containing vitamine-A aldehyde retinal (Fig. 1A) as a chromophore are generally called "Retinal (or Retinylidene) proteins" [1]. These retinal proteins have basically been classified into two groups, microbial (type-1) and animal (type-2) proteins [1,2]. In both types retinal works as a chromophore within the opsin. This article focuses on structure-function relationship among type-1 retinal proteins.

In 1971, a retinal protein has been found in the halophilic archaeon *Halobacterium salinarum* (formerly *halobium*) by Drs. Oesterhelt and Stoeckenius [3] (Fig. 1A). Similar to the visual rhodopsins, this molecule named bacteriorhodopsin (BR) is an integral membrane protein having both seven-transmembrane α-helices and a retinal chromophore linked to a specific lysine residue (Lys216) via a protonated Schiff base (PSB) linkage (Fig. 1A) [4]. Several sites in this protein have been of major attention in the research discussed in this review and those are shown in Fig. 1B with the alignment of putative amino acid sequences of other microbial type-1 retinal proteins. Most of them have an arginine and two aspartate residues at the position of BR Arg82, Asp85 and Asp 212. These residues and PSB form a quadrupole structure called "pentagonal cluster" [5], and it would be important for the structural stability of type-1 rhodopsins. BR acts as a light-driven outward proton pump across the membrane, and such a proton gradient is utilized by the ATP (adenosine triphosphate) synthase, indicating that organisms having light-driven pumps can produce ATP under light illumination [6,7]. It is well-known that ATP is a multifunctional nucleotide, used in cells and organisms as a coenzyme, and is often called the molecular unit of currency of intracellular energy transfer. In the past four decades since its discovery, BR has become a model for the simplest and most essential features necessary in an active proton transporter that is activated by a light stimulus. It should be noted that until recently, BR and related proteins capable of producing a chemiosmotic membrane potential in response to light had only been described in halophilic archaea [6].

In 2000, however, a type of retinal protein derived from γ-proteobacteria was discovered through genomic analysis in marine bacterioplankton, and was named "Proteorhodopsin (PR)" (Fig. 1A) [8]. PR exhibited a photocycle with intermediates and kinetics characteristic of BR, and showed active proton transport upon photoillumination. Since then, thousands of PR-like proteins have been discovered mainly from marine environment. This implies that archaeal-like retinal proteins are broadly distributed among different taxa, including members of the domain bacteria. Moreover, in 2005, a fungal retinal protein (*Leptosphaeria* Rhodopsin: LR) was found and identified from the eukaryota *Leptosphaeria maculans* (Fig. 1A) [9]. LR turned out to be very similar to BR in its photochemical behavior, and exhibits light-driven active proton transport. At present, a vast number of microbial type-1 retinal proteins, such as *Acetabularia* Rhodopsin (AR) [10], xanthorhodopsin (XR) [11], *Gloeobacter* Rhodopsin (GR) [12],

Abbreviations: BR, bacteriorhodopsin; HR, halorhdopsin; SRI, sensory rhodopsin I; SRII, sensory rhodopsin II; MR, middle rhodopsin; ASR, *anabaena* sensory rhodopsin; AR3, archaearhodopsin-3

☆ This article is part of a Special Issue entitled: Retinal Proteins - You can teach an old dog new tricks.

* Corresponding author at: Division of Biological Science, Graduate School of Science, Nagoya University, Nagoya 464–8602, Japan. Tel.: +81 52 789 2993; fax: +81 52 789 3054.
E-mail address: z47867a@cc.nagoya-u.ac.jp (Y. Sudo).

0005-2728/$ – see front matter © 2013 Elsevier B.V. All rights reserved.
http://dx.doi.org/10.1016/j.bbabio.2013.05.005

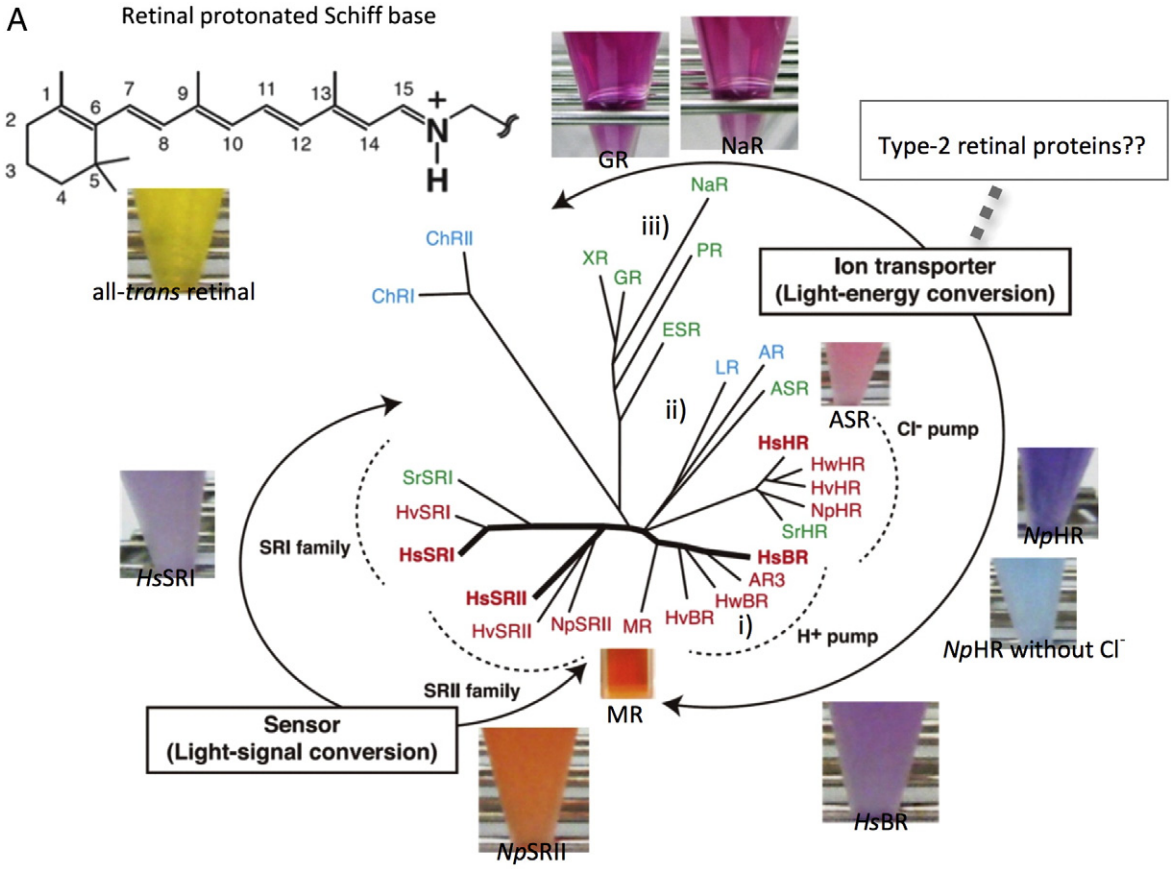

B

HsBR	82	85	96	125	128	141	144	145	176	177	185	193	194	200	204	205	210	211	212	215	216	223	226
(NpSRII)	(72)	(75)	(86)	(105)	(108)	(130)	(133)	(134)	(165)	(166)	(174)	(182)	(183)	(189)	(193)	(194)	(199)	(200)	(201)	(204)	(205)	(211)	(214)
(SrSRI)	(69)	(72)	(83)	(102)	(105)	(127)	(130)	(131)	(162)	(163)	(171)	(179)	-	(185)	(189)	(190)	(195)	(196)	(197)	(200)	(201)	(208)	(211)
HsSRI	R	D	Y	D	M	S	F	H	N	H	Y	P	A	T	V	A	F	L	D	A	K	F	R
HvSRI	R	D	F	D	M	S	F	H	N	H	Y	P	E	T	V	S	F	L	D	A	K	F	R
SrSRI	R	D	Y	D	M	A	C	H	N	H	Y	P	-	S	V	S	Y	M	D	A	K	V	S
HsSRII	R	D	Y	D	V	G	G	Y	N	I	Y	P	A	Q	Y	T	Y	L	D	S	K	A	G
NpSRII	R	D	F	N	V	G	A	F	N	L	Y	P	P	T	D	V	Y	L	D	T	K	I	D
ASR	R	D	S	Q	V	G	A	F	T	Y	Y	P	S	N	D	T	L	L	P	S	K	D	G
HsBR	R	D	D	D	M	S	A	M	N	V	Y	S	E	P	E	T	V	L	D	A	K	L	S
HsHR	R	T	A	D	M	S	F	F	V	L	Y	V	E	Q	V	T	V	L	D	A	K	L	W
NpHR	R	T	A	D	M	S	C	F	L	L	Y	V	E	P	Y	T	A	L	D	A	K	L	Y

Fig. 1. A) Chemical structure of the all-*trans* retinal protonated Schiff base and diversity of microbial type-1 retinal proteins. Retinal proteins show various colors, and exhibit two basic functions, the light-energy conversion and light-signal conversion. They widespread in archaea (red), eubacteria (green) and eukaryotes (blue). B) Alignments of some amino acid residues in type-1 retinal proteins. BR, SRII and SRI on the top of the panel indicate the molecules from *H. salinarum*, *N. phraonis* and *S. ruber*, respectively, with the numbers of their amino acid residues.

Exiguobacterium sibiricum Rhodopsin (ESR) [13,14] and sodium pump rhodopsin (NaR) [15] have been found in the genomes of many organisms except for higher plants and animals (Fig. 1A). Thus, it is now obvious that BR and related proteins are very common for large taxonomic groups within the three biological kingdoms, eukarya, bacteria and archaea (Fig. 1A), indicating that in many organisms the proton gradient produced by proton pumps could be utilized by the ATP synthesis, generating biochemical energy from light. The phylogenic analysis implies that these proton pumps are categorized to a few distinct clades including i) BR (*Hs*BR), AR3 (archaerhodopsin-3) and their related proteins, ii) fungal rhodopsins such as LR and iii) PR, XR, ESR and their related proteins, and they locate far from each other (Fig. 1A). All of proton-pumping rhodopsins have conserved carboxylic residues at the positions of BR Asp85 and Asp96 (Fig. 1B). Both of them are important for the proton transport and they function as a proton acceptor and a donor for the retinal Schiff base in the photoreaction of proton-pumping rhodopsins.

In 1977, a second retinal protein named halorhodopsin (HR) has been discovered in the archaeon *H. salinarum* by Drs. Matsuno-Yagi and Mukohata (Fig. 1) [16]. Dr. Lanyi et al. has demonstrated that HR acts as a light-driven inward chloride pump [17]. Functionally, HR is the mirror image of BR: anions such as Cl^-, Br^- and I^- instead of cations are transported, and the translocation is in the extracellular → cytoplasmic direction [18]. An aspartate at the position of Asp85 in BR is replaced by threonine in HR (Fig. 1B). This aspartate is a member of the electric quadruple in other rhodopsins, and the quadruple structure is maintained by the binding of an anion in HR [19]. In 1995, Dr. Sasaki and coworkers reported that the replacement of a single amino acid residue converts BR from a proton to a chloride pump, which implies that the essential

features of the proton transport mechanism of BR are commonly conserved in the anion transport mechanism of HR [20]. Similar to BR, HR-like retinal proteins are widely distributed both in archaea and bacteria (Fig. 1A), indicating that the light-energy conversion by chloride pumping is for various microorganisms also important to survive in nature. Thus, light-driven ion transport is one of the major biological functions among type-1 retinal proteins (Fig. 1A).

Is there any relationship between type-1 and type-2 retinal proteins? The configuration of the retinal chromophore and its isomerization are different between type-1 and type-2 retinal proteins. All-*trans* (or 13-*cis*) retinal irreversibly binds to the opsin in the case of type-1 proteins, and isomerizes to 13-*cis*, whereas 11-*cis* (or all-*trans*) retinal reversibly binds to the opsin for type-2 and isomerizes to all-*trans* (or 11-*cis*) [2]. In addition to this, the tertiary structures of type-1 retinal proteins including BR and HR are less similar to those of type-2 retinal proteins such as bovine rhodopsin and squid rhodopsin, although the proteins are commonly constructed by seven-transmembrane α-helices [21]. On the other hand, type-1 retinal proteins with the cytoplasmic loop of bovine rhodopsin have been shown to significantly activate the trimeric G-protein transcucin similar to type-2 retinal proteins [22,23]. Furthermore, a type-1 retinal protein named middle rhodopsin (MR) has been discovered that has 11-*cis* retinal as a chromophore similar to type-2 retinal proteins [24]. Recently, Drs. Koyanagi and Terakita found that a type-2 retinal protein named Opn3 acts as a light sensor when constituted with 13-*cis* retinal similar to type-1 retinal proteins such as BR and HR [25]. In addition, the sequence similarity between microbial type-1 retinal proteins and metazonal type-2 retinal proteins has been pointed out by phylogenetic analysis [26]. Thus, the evolutionary relationship between type-1 and type-2 retinal proteins is still an interesting open question (Fig. 1A).

1.2. Conversion of light energy into signal with microbial rhodopsins

Another major function of microbial retinal proteins is light-signal transduction. A third retinal protein, named sensory rhodopsin I (SRI), has been discovered in the archaeon *H. salinarum* in 1982, and it has been shown to regulate both positive and negative phototaxis (Fig. 1A) [27]. In 1985, a fourth retinal protein was discovered in *H. salinarum*, and the function of this molecule has been identified as a sensor for negative phototaxis (Fig. 1A) [28]. This retinal protein was named sensory rhodopsin II (SRII or phoborhodopsin, pR). In this review article, we would like to focus on the molecular mechanism of the light-signal transduction by these sensory rhodopsins and their related proteins mainly based on our recent results together with other findings reported by researchers including Drs. Naoki Kamo, John L. Spudich, Dieter Oesterhelt and Martin Engelhard.

2. The dawning of microbial sensory rhodopsins

Motile organisms on earth such as bacteria and archaea are accustomed to survive in the various environments in which they live, by changing their swimming mode to migrate toward more favorable habitats or to avoid more harmful habitats. This behavior, termed *taxis*, is achieved by a signaling system from membrane-embedded receptors (input) to the flagellar motor (output) [29]. Light is one of the most important signals providing critical information to biological systems, and therefore, many organisms utilize light, not only as an energy source, but also as a signal [30]. The phototaxis of *H. salinarum* was the first to be described, and those cells show both positive and negative phototaxis. The light stimulus is captured by the photoreactive membrane-embedded retinylidene proteins, SRI and SRII (Fig. 2). In the cell membranes, SRI and SRII form complexes with their cognate transducer proteins, called Halobacterial transducer protein for SRI (HtrI) and for SRII (HtrII), respectively, (Fig. 2) [30,31]. Light signals are transmitted from the SRI-HtrI and SRII-HtrII complexes to a cytoplasmic two-component signal transduction cascade, consisting of the kinase CheA and the response regulator CheY, which regulates the rotational direction of the flagellar motor, resulting in positive or negative phototaxis (Fig. 2). Such stimulus-induced changes in the motility of cells are well-characterized in the case of chemoreception in bacteria. Especially the chemotaxis behavior in two bacterial species, *Escherichia coli* and *Salmonella enterica* has been extensively studied (for reviews) [32–34].

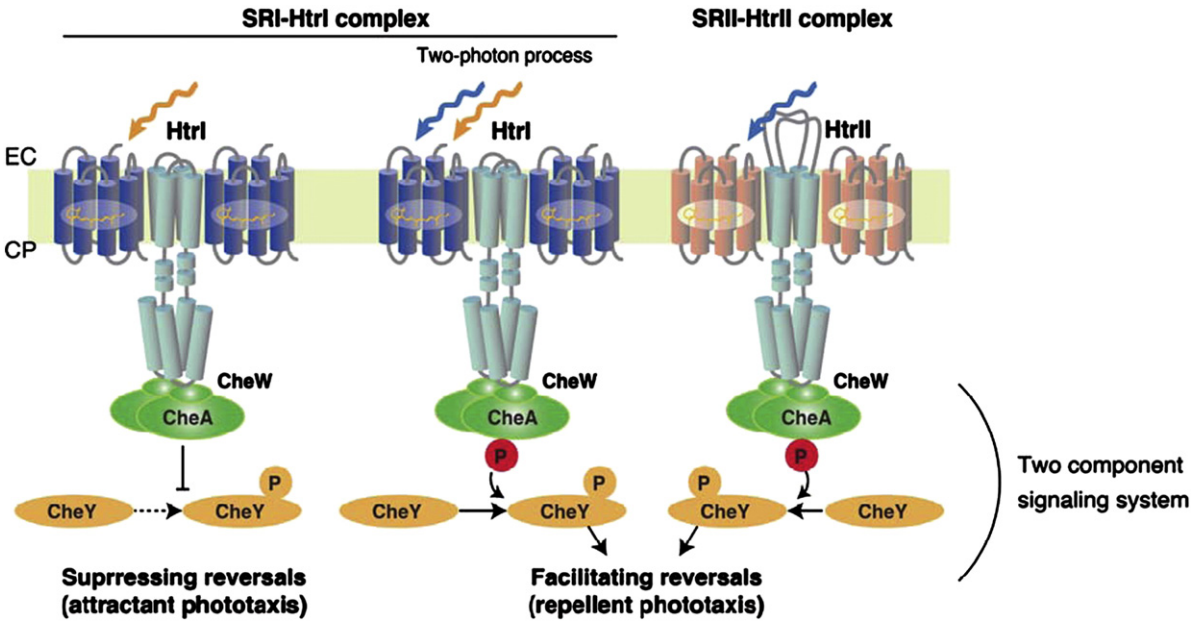

Fig. 2. Sensory rhodopsins, photo-attractant sensory rhodopsin I (SRI) and photo-repellent sensory rhodopsin II (SRII, also known as phoborhodopsin, pR), responsible for the phototaxis responses. Cognate halobacterial transducer proteins, HtrI and HtrII, for SRI and SRII are also illustrated, respectively. SRI absorbs green-orange light and induces an attractant phototaxis response to help to activate the ion-pumps. SRII absorbs blue light, and induces a repellent phototaxis response to keep away from harmful UV radiation. The cells then adjust to the new light intensity and resume their prestimulus reversal frequency (adaptation).

2.1. Sensory rhodopsin I

Light absorption by SRI from *H. salinarum* (*Hs*SRI) triggers the *trans-cis* photoisomerization of the retinal chromophore, leading to its photocycle (Fig. 3A). During this photocycle, *Hs*SRI passes through the following photoreaction scheme; SRI(587) → K(620) → L(540) → M(373, also known as S_{373}) → SRI(587) [30]. The numbers denote the wavelengths of the maximum absorption of the respective intermediates. The M intermediate is the active state for the positive phototaxis. When light around 587 nm illuminates the protein, and the M intermediate is formed, the *H. salinarum* cells swim toward the light. However, when the illuminating light contains also near-UV radiation, the cells turn around to keep away from the harmful light [35]. This near-UV light is sensed by the blue-shifted M intermediate. Once the M intermediate absorbs near-UV light, a photo-intermediate called P_{520}, which induces the repellent phototaxis signals, is formed via the following reaction scheme; M(373) → P(520) → SRI(587) (Fig. 3A) [30]. Therefore, P(520) is thought to be the photo-repellent signaling state. Thus, *Hs*SRI is a dual photoreceptor for two opposite functions, the positive and negative phototaxis (Fig. 2A). Furthermore, a close relationship between the transport and sensory signaling activities of microbial type-1 retinal proteins has been revealed when *Hs*SRI was separated from its tight complex with HtrI, and was found to exhibit light-driven electrogenic proton transport across the membrane [36,37]. Thus, this transport activity of *Hs*SRI is blocked by HtrI binding [36,37].

2.2. Sensory rhodopsin II

The fourth rhodopsin-like pigment in *H. salinarum* was discovered by Dr. Takahashi and coworkers in 1985 [28,38]. They isolated the *H. salinarum* mutant which lacks BR, HR, and SRI, but shows a repellent phototaxis response whose sensitivity maximum was at around 480 nm. In 1986, two groups [39,40] independently characterized the fourth pigment. One group named it "phoborhodopsin (pR)" because of the photophobic behavior of the mutant strain, but it is essentially a second sensory rhodopsin, and therefore, it is also called sensory rhodopsin II (SRII). SRII (pR, $\lambda_{max} = 487$ nm) from *H. salinarum* (*Hs*SRII) is activated by blue light and produces only a repellent phototaxis signal, whereas *Hs*SRI produces both attractant and repellent signals as described above. In the native *H. salinarum* cell membrane, the expression level of *Hs*SRII is the lowest among the four pigments (ca. 1/10–1/1000). In addition to this, the protein stability is significantly low in the presence of detergents and/or under low salt concentration. Therefore photochemical properties of SRII have mainly been investigated by using membrane fragments [41–46]. The estimated photocycle of *Hs*SRII is essentially; SRII(487) → M(~360) → O(~525) → SRII(487) (Fig. 3B). The M and O intermediates are thought to be the signaling state(s) for the photo-repellent cell behavior [47]. In addition to these two sensory rhodopsins, SRI and SRII, a third sensory rhodopsin molecule (named sensory rhodopsin III, SRIII) has been recently found in the halophilic archaeon *Haloarcular marismortui*, although its function has not been identified,

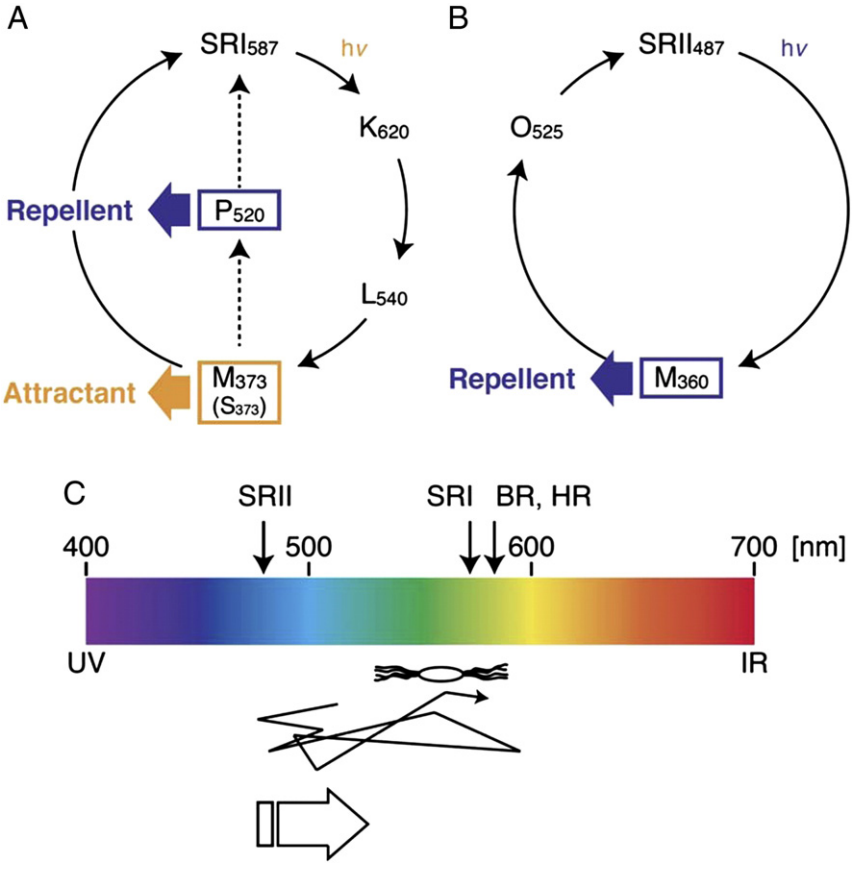

Fig. 3. Photochemical reaction cycles of SRI (A) and SRII (B) both from *H. salinarum*. *Hs*SRI absorbs green-orange light and forms K_{620}, L_{540}, and M_{373} intermediates, from which M_{373} is the attractant signaling state. When near-UV light shines onto the M intermediate, the P520 intermediate is formed to produce a repellent phototaxis signal. *Hs*SRII absorbs blue light and forms K_{540}, L_{488}, M_{390}, and O_{560}. The M_{390} state is the repellent signaling state. C) Color discrimination in the archaeon *H. salinarum*. The cells are attracted to light with wavelengths longer than 520 nm, and avoid light shorter than 520 nm by SRI and SRII. Light of >520 nm can activate BR and HR to obtain the light-energy, and cells avoid the shorter wavelength light, which contains harmful near-UV.

yet [48]. Thus, similar to vision in vertebrates, microorganisms can also sense light; they show avoidance or attractive behavior from or toward light of certain wavelengths [30]. Thus, *H. salinarum* is attracted to light with wavelengths longer than 520 nm, and avoids light shorter than 520 nm. Light of >520 nm can activate BR and HR for light-energy conversion, while cells avoid light of shorter wavelengths, which contains harmful near-UV radiation (Fig. 3C).

3. Molecular mechanism for the negative phototaxis initiated by SRII

3.1. A high stable homolog from Natronomonas pharaonis

Seven years after the discovery of SRII from *H. salinarum* (*Hs*SRII), a second sensory rhodopsin II homolog has been isolated and partially purified from the archaeon *Natronomonas pharaonis* (formerly *Natronobacterium pharaonis*) by Drs. Hirayama and Kamo in 1992 [49]. When the protein *Np*SRII is expressed in *H. salinarum* cells with its cognate transducer protein *Np*HtrII, the cells shows a negative phototaxis response similar to cells expressing *Hs*SRII-*Hs*HtrII [50], indicating that *Np*SRII and *Np*HtrII are functionally homologous proteins of *Hs*SRII and *Hs*HtrII. In 1997, Drs. Shimono and Kamo have succeeded in the functional expression of *Np*SRII in the membrane of *Escherichia coli* cells as a recombinant protein [51] (Fig. 4). This is the first type-1 retinal protein, which could be functionally expressed in *E. coli*. After that, the truncated *Np*HtrII form which has both two transmembrane domains and a partial cytoplasmic region has also been expressed in *E. coli* cells [52]. In 2007, the expression of full-length *Np*HtrII in *E. coli* cells has also been reported [53]. In addition to the favorable expression system, the high stability of *Np*SRII and *Np*HtrII even in detergent micelles and dilute salt solutions [54,55] made it possible to prepare large amounts of protein, and enabled studies of mutant proteins that allowed new approaches to investigate the photosignaling process of SRII. In fact, the crystal structures of *Np*SRII have been reported by two independent research groups in 2001 [56,57]. Although ~74% of residues in *Np*SRII differ from those of BR and HR, their crystal structures show close similarities in architecture, helix positions and locations of the retinal-binding pocket (RMSD of Cα = ~1.5 Å) [4,19,56,58], indicating that their functional differentiation is regulated by differences in more detailed structures including the amino acid side chain(s), ions and water molecules. Thus, despite their high similarity in structure, the question arises of how these proteins can function so differently?

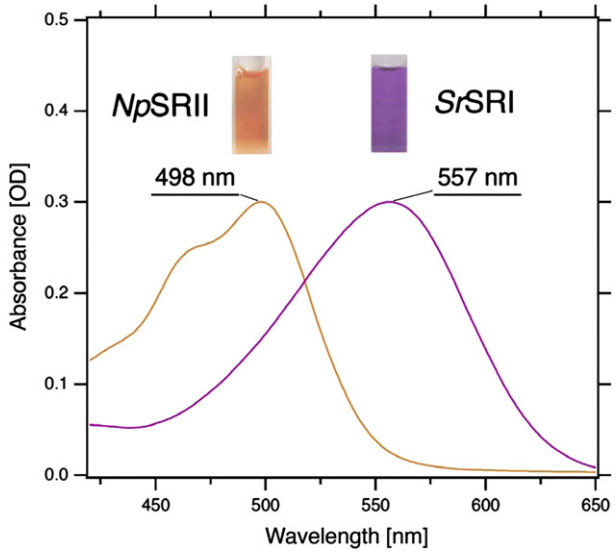

Fig. 4. Visible absorption spectra of the purified *Np*SRII and *Sr*SRI. These proteins were expressed in *E. coli* cells as recombinant proteins, purified by column chromatography and suspended in a buffer containing 1 M NaCl, 50 mM Tris – Cl pH 7.0 and 0.05% DDM.

3.2. Photochemical properties of NpSRII

From spectroscopic studies, it has been revealed that there are some significant differences between ion pumping rhodopsins (BR and HR) and *Np*SRII: i) Retinal configuration, ii) Absorption maximum and iii) Photocycling rate.

i) Retinal configuration; The retinal configuration of *Np*SRII was studied by a chromophore extraction method with hydroxylamine followed by HPLC analysis. The results showed that *Np*SRII binds only the all-*trans* isomer (~100%) both in the dark and under light conditions [59], whereas BR and HR have two isomers, all-*trans* and 13-*cis*, with approximately 1:1 ratio, in the dark [7,60]. This makes the photochemical study on the dynamics of *Np*SRII easier, because there is no prolonged accumulation of the 13-*cis* form. From experiments using retinal analogs, it has been suggested that the space of the retinal binding pocket of *Np*SRII is less restricting for the retinal chromophore, compared with BR [61]. However, further explanations are required because the structure around the retinal chromophore of *Np*SRII is highly similar to that of BR.

ii) Absorption maximum; *Np*SRII has a ca. 60 nm blue-shifted absorption spectrum (λ_{max} = 498 nm) compared with BR, HR and SRI, and it shows a characteristic shoulder peak at around 470 nm (Fig. 4) [49,62]. In general, colors of proteins originate from the energy gap between the ground and excited states. The observed fine structure was theoretically explained by the vibronic coupling between the S_1 and S_2 states of the retinal [63,64]. First, it was expected that the color difference between BR and SRII could be explained by their relatively large structural difference(s). However, as mentioned above, the crystal structure of *Np*SRII is surprisingly highly similar not only to BR, but also to HR. Thus, it is obvious that the color tuning must be achieved by considerably small structural difference(s) (<1.5 Å). On the basis of the crystal structures of SRII and BR, the color tuning mechanism has been investigated theoretically [63,64], while we analyzed it experimentally. In 2001, we prepared several *Np*SRII mutants in which each residue was replaced by its corresponding residue in BR [65]. Even a 10-point replacement of amino acid residues located within 5 Å of the retinal cannot account sufficiently for the difference: the λ_{max} of this mutant red-shifted only to 524 nm but not around to 550 nm where the λ_{max} of BR locates when it is expressed in *E. coli* cells and measured in detergent micelles (Fig. 5A). A further study using chimeric proteins between *Np*SRII and BR pointed out the importance of the broad regional interaction, mainly between helices D and E, for the spectral tuning of *Np*SRII [66] (Fig. 5A). Thus, from these results, we concluded that three residues, Val108, Gly130 and Thr204, and the D-E interaction are the key factors for the spectral tuning between *Np*SRII and BR (Fig. 5B) [66].

iii) Photocycling rate: The primary photoreaction process of *Np*SRII has been studied by ultrafast transient absorption [67] and picosecond ultraviolet resonance Raman (UVRR) spectroscopy [68] (Fig. 6). Compared with *Hs*SRII (Fig. 3B), the photocycle kinetics of *Np*SRII is well-characterized. Transient absorption measurements observed a transition between two red-shifted intermediates within 5 ps after the relaxation of the electronic excited state in 300–400 fs. The former red-shifted intermediate could be identical to the J intermediate observed in the photocycle of BR which has highly twisted C – C and C═C bonds on the retinal polyene chain [69], and J then converts to the second red-shifted intermediate, K, within 5 ps. UVRR spectroscopy observed the reduction of the intensity of Raman bands of tryptophan and tyrosine residues within the instrumental response time, followed by their recovery with a time constant of 30 ps. The former reduction could be assigned to the production of J, and we suggested that the

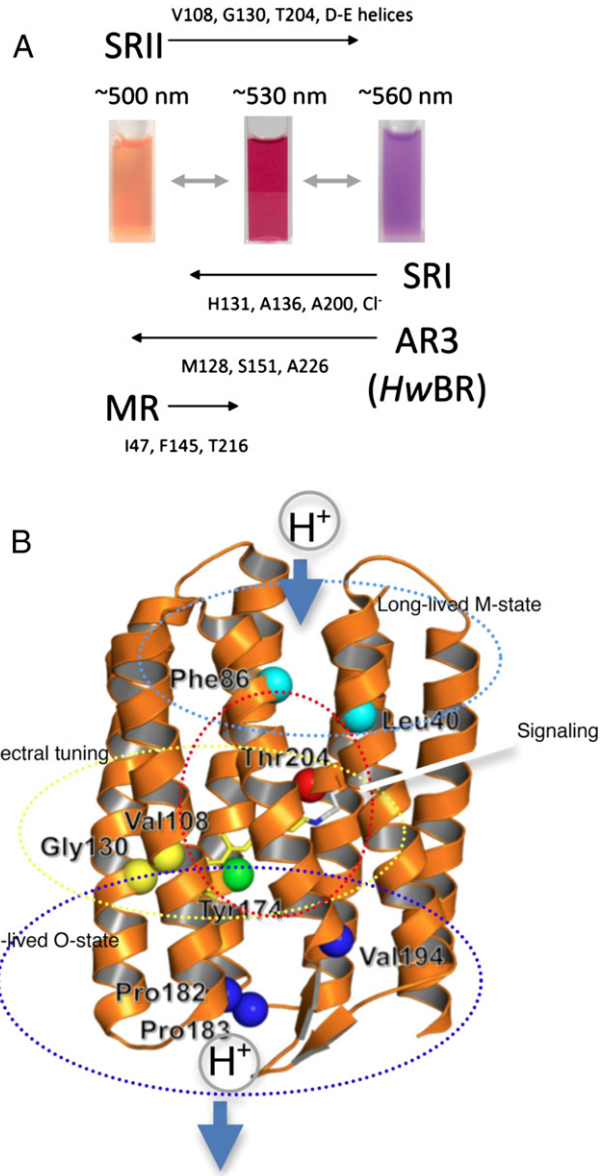

Fig. 5. (A) Important color tuning residues (region) among microbial type-1 retinal proteins. (B) Responsible residues for the color tuning (yellow), the slow photocycle (cyan and blue) and the signaling (red) in *Np*SRII.

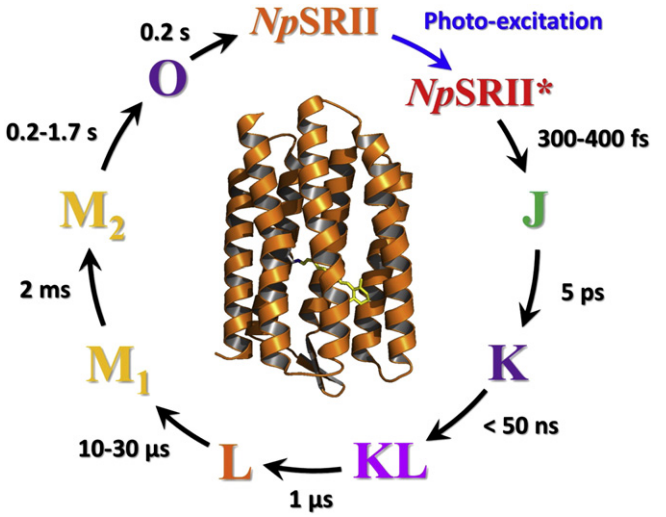

Fig. 6. Photocycle of *Np*SRII based on the results of various time-resolved measurements [71–75]. An asterisk represents the electronically excited state.

latter recovery represents the formation of a "post-K" state. Femtosecond time-resolved mid-infrared spectroscopy also observed the change of bands at 1550 and 1530 cm^{-1} in 11 ps attributed to the change of the amide-II bands of the protein backbone [70], and this component could represent the same process observed in UVRR study, thus, the formation of the post-K state. Although, the time constants are slightly different to those of BR, the primary photoreaction process of *Np*SRII in the femoto- to picosecond time region is quite similar. The photocycle in the time-region longer than a nanosecond has been studied by various researches with laser flash photolysis and other time-resolved techniques [71–75]. Although the kinetics suggested by each research group showed some differences from each other, the overall aspects coincided, and the K, KL, L, M_1, M_2, and O intermediates were identified in the photocycle of *Np*SRII (Fig. 6). While most of the intermediate were shown to bind 13-*cis* retinal, the O state of *Np*SRII has all-*trans* retinal analogous to the BR photocycle [76].

One of the differences to BR and HR is the photocycling rate. Ion-pumping rhodopsins, such as BR and HR, have been optimized by nature to have relatively fast photocycling rates (~10 ms), making them efficient pumps, whereas the sensory rhodopsins, SRI and SRII, have slow photocycles, persisting for several seconds, which allow the transient accumulation of long-lived signaling states (M and/or O intermediate) of the receptors to catalyze a sustained phosphorylation cascade. The slow photocycle of sensory rhodopsins is thought to be caused by the lack of an aspartate, Asp96 in BR, which works as a proton donor at the M state (Fig. 1B) [77]. The M-decay of *Np*SRII was strongly accelerated by the addition of azide similar to that in the D96N mutant of BR in which Asp96 was substituted by Asn, and the M-decay rate was comparably slow due to the lack of an internal proton-donating group (Asp96) to the deprotonated Schiff base of the M intermediate [78]. In *Np*SRII, the analogous donor is also absent: the residue corresponding to Asp96 of BR is Phe86 (Fig. 5B), which probably explains at least partially the slow decay of $NpSRII_M$. The addition of azide increased the rate of the $NpSRII_M$-decay dramatically [79]. Furthermore, in a double mutant of *Np*SRII, F86D/L40T, in which the internal proton donor and possibly the hydrogen-bonding network was restored, the M-decay was accelerated as much as approximately 130-fold at pH 7.0, making it almost equal to that of BR [80]. On the other hand, the long-lived O-intermediate was still observed in this mutant with a similar rate constant to that in the wild-type [80]. It should be mentioned that all of the sensory rhodopsins discovered so far do not have a carboxylic residue at this position (Fig. 1B). Thus, the long-lived M-intermediate of sensory rhodopsins can be assumed to be achieved by the lack of the proton donor in the cytoplasmic (CP) channel (Fig. 5B) [81].

Analogous to BR, the $NpSRII_O$-decay coincides with the proton transfer from the protonated counterion of the PSB, Asp75, to the proton releasing group (PRG) at the extracellular surface through an extracellular proton conduction channel. A comparison of the amino acid alignment of BR and *Np*SRII [82] in this extracellular (EC) channel suggests a higher hydrophobicity for *Np*SRII than BR. Here, the hydrophilic residues of Ser193, Glu194 and Thr205 in BR are replaced by Pro182, Pro183, and Val194 in *Np*SRII, respectively, but the negative charge of Glu204 is conserved as Asp193 (Figs. 1B and 5B). In addition to these three amino acid residues, Dr. Klare et al. noted that Thr204 in *Np*SRII influences the O-decay [83]. Therefore, we prepared various multiple mutants of these four residues. As a result, the decay of $NpSRII_O$ of the quadruple mutant (SETC) was accelerated ~100-times from 690 ms for the wild-type to 6.6 ms for the mutant, making it almost equal to that of BR [84]. Thus, we concluded that the long-lived O-intermediate in *Np*SRII is also achieved by the inhibition of the proton translocation in

the EC channel (Fig. 5B) [84]. While most of the process is not affected by the binding of *Np*HtrII, the decay rate of M_2 becomes 2-fold slower in the complex [52]. It should be noted that this observation is only valid for solubilized *Np*SRII–*Np*HtrII complex. In purple membrane lipids (native) the binding of *Np*HtrII does not change the kinetics of *Np*SRII [85].

Dr. Siebert's group studied the photocycle of *Np*SRII by time-resolved FTIR [86]. They obtained the intermediate spectrum of K which was similar to that trapped at low-temperature. While the change between K and L was relatively small, protonation of Asp95 and larger change of amide bands were observed on the M intermediate. Then, *Np*SRII converted to the O intermediate with the signals of retinal reisomerization. In the presence of azide, the decay of M was accelerated and another red-shifted intermediate containing 13-*cis* retinal (the MO state) was identified after the M-decay. The rate of reisomerization was still slower even in the presence of azide. This indicates that the rate of reisomerization is not determined by the protonated state of the Schiff base.

3.3. Interaction with cognate transducer protein HtrII

We and Dr. Engelhard's group demonstrated independently that *Np*SRII forms a complex with *Np*HtrII in both detergents and the membrane with a 1:1 stoichiometry [52,87], and a 2-fold symmetric 2:2 complex is stably observed in the lipid membrane [85,88,89]. The crystallographic structure of *Np*SRII revealed the interaction surface with *Np*HtrII. A residue Tyr199 is located at the lipid-facing surface of helix-G. Tyr199 is completely conserved among SRII proteins, but it is replaced by Val for *Hs*BR and Phe for *Hs*SRI (Fig. 1B). In addition, the O-H group of Tyr199 is thought to be energetically unfavorable within the membrane because of its hydrophilicity. To investigate the role of Tyr199 on the interaction with *Np*HtrII, we developed a method to determine the dissociation constant (K_d) on the basis of the effect of the interaction on the decay rate of the O-like state [52,90]. The K_d value of the Y199F or Y199V mutants with *Np*HtrII was ~10-fold larger than that without mutation, showing the significant contribution of the O-H group of Tyr199 to the binding [91]. In 2002, the X-ray crystallographic structure of the *Np*SRII/*Np*HtrII complex was obtained at 1.93 Å resolution by Dr. Gordeliy and coworkers [89] (Fig. 7A). The structure revealed that Tyr199 of *Np*SRII formed a hydrogen bond with Asn74 on the second transmembrane helix (TM-2) of *Np*HtrII (Fig. 7A). Another hydrogen bonding network composed of Thr189 of *Np*SRII and Glu43/Ser62 of *Np*HtrII was revealed in the interaction surface between *Np*SRII and *Np*HtrII (Fig. 7A). The two hydrogen bonding networks (Tyr199/Asn74 and Thr189/Glu43/Ser62) are considered to be critical for the strong interaction of *Np*SRII and *Np*HtrII because the double mutation of Thr189 and Tyr199 of *Np*SRII (T189V/Y199F) 62-fold increases the K_d (0.16 μM and 9.9 μM for wild type and T189V/Y199F, respectively) [92]. Furthermore, it has been shown that BR and HR which originally cannot bind with *Np*HtrII become able to bind with it when hydrogen bond-forming amino acid residues are introduced at the proper positions of BR and HR, which clearly indicates that these two hydrogen bonds play important roles in the binding. It should be however noted that even the hydrogen-bondless mutant of SRII (T189V /Y199F) has a binding activity with *Np*HtrII (K_d = 9.9 μM) [92]. Of interest, the BR and HR mutants having hydrogen bonding residues bind with HtrII (K_d = 29–60 μM) however weaker than does the T189V /Y199F mutant of *Np*SRII (K_d = 9.9 μM) [92]. These results suggest that hydrophobic and/or van der Waals interaction is also involved in the binding. It should be noted that the X-ray structure shows intimate contact between SRII and HtrII; The helix-TM2 of HtrII is nested in the groove formed by helices-F and G of SRII. In addition to the transmembrane region it is revealed from solution NMR spectroscopy and calorimetric analysis that the cytoplasmic region of *Np*HtrII termed HAMP (histidine kinases, adenylyl cyclases, methylaccepting chemotaxis proteins, and phosphatases) domain participates in the interaction with SRII [93].

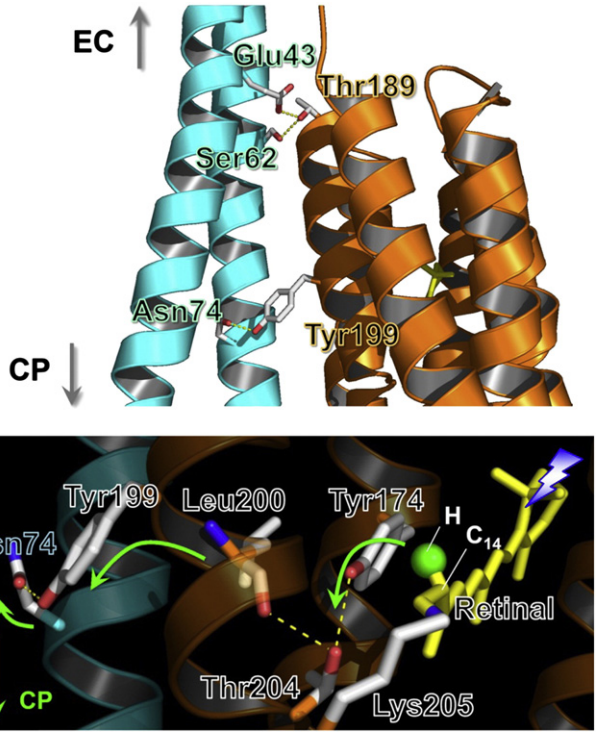

Fig. 7. (A) Hydrogen bonding network at the interface between *Np*SRII (orange) and *Np*HtrII (cyan). These interactions stabilize the *Np*SRII/*Np*HtrII complex. The side chains of the residues forming the hydrogen bonds between the molecules were shown by a stick model and yellow dashed lines represent the expected hydrogen bonds. (B) Constraint of C_{14}-H of the retinal upon the photo activation and the network of the functionally important residues. The steric constraint between the retinal C_{14} group and the side chain of Thr204 has a positive correlation with the efficiency of the phototaxis responses, and this constraint is considered to cause a perturbation to the hydrogen bonding network between Tyr174, Thr204 and the main-chain carbonyl of Leu200. Finally, the steric perturbation is transferred to Asn74 on helix-F of *Np*HtrII via Tyr199. Because most of these residues are indispensable for the phototaxis signaling, the photo-induced interaction among them is one of the key mechanisms of the signal transduction between the activated *Np*SRII and *Np*HtrII.

Furthermore, the replacement of Asp193 on helix-G of *Np*SRII which locates in the homologous position of Glu204 in BR, which is known as the proton releasing group, inhibits the complex formation [94]. In the crystallographic structure, Asp193 interacts with Arg72, and the disruption of this electrostatic interaction seems to affect the formation of the complex. In the vicinity of Arg72, the binding of a Cl^- ion was observed [57]. Although the physiological significance of this Cl^- ion is unknown, low-temperature- and attenuated total reflection (ATR)-FTIR studies revealed that it is released from the binding side together with the H^+ release from Asp193 to the extracellular side upon formation of the M intermediate [95]. The apparent *pKa* value of Asp193 in the ground state and the M state of *Np*SRII was determined to be 6.4 and 4.9, respectively, and it decreased to 5.6 and 3.9, respectively, in the complex with *Np*HtrII [84]. Thus, both inter- and intramolecular contacts between *Np*SRII and *Np*HtrII are involved in the interaction.

3.4. Structural changes during the photocycle

The structural changes during the photocycle of *Np*SRII have been investigated by using low-temperature FTIR spectroscopy. Illumination of *Np*SRII below −100 °C produced an intermediate corresponding to the K intermediate of BR, and this intermediate has been denoted $Np\text{SRII}_K$ [42]. We trapped $Np\text{SRII}_K$ at 77 K, and compared the $Np\text{SRII}_K$ minus *Np*SRII spectra in the presence and absence of *Np*HtrII [96,97]. This difference spectrum showed clear differences for the amide-I and amide-A vibrations, indicating that the complex

formation affects the structure of the peptide backbone. In ion pumping rhodopsins such as BR and HR, chromophore distortion upon formation of the K intermediate are localized in the Schiff base region (see Fig. 1A), as shown in their hydrogen out-of-plane (HOOP) vibrations. In contrast, more extended structural changes take place in *Np*SRII$_K$ in view of chromophore distortion and protein structural changes both in the presence and absence of *Np*HtrII. In addition, we found D_2O insensitive X-H vibrational bands of *Np*SRII at 3479(−)/3369(+) cm^{-1} that were observed only in the presence of *Np*HtrII [98]. Because these positive and negative bands disappeared in the T204A mutant, and shifted in the T204S mutant [98], we concluded that the bands originate from the O-H stretch of Thr204 in *Np*SRII. The large spectral shift ($\Delta = 110\ cm^{-1}$) indicates a strong hydrogen bonding alteration upon photoisomerization of the retinal (Fig. 7B).

In 2005 [99], we showed that the intensity of the C_{14}–D stretching vibration band of deuterated retinal is dramatically enhanced upon the formation of the K intermediate. This was interpreted as indicating a steric constraint of the C_{14}–D group by Thr204 (Fig. 7B), because the C_{14}–D stretching signal disappeared in the T204A, T204S, and T204C mutants similar to the C_{14}-HOOP vibration at 864 cm^{-1} [100]. Thr204 forms a hydrogen bonding network with Tyr174 and the main chain carbonyl of Leu200. The steric constraint indicates that an energy flow occurs from the distorted chromophore to this network. A comparison between the UVRR spectra of the WT and Y174F mutant of *Np*SRII indicates that Tyr174 changes its structure and/or environment upon chromophore photoisomerization [68]. Because Tyr174 is known to form a hydrogen bond with Asp201 and Thr204, the result implies the presence of an energy flow from the isomerized retinal to Tyr174, Asp201 and Thr204 (Fig. 7B).

Then we analyzed the structural changes in the functionally important intermediates, M and O. We previously demonstrated that the association of *Np*SRII and *Np*HtrII is 2-orders of magnitude weakened upon M-formation [101,102]. Low-temperature and rapid-scan FTIR studies showed that the hydrogen bond between Tyr199 of *Np*SRII and Asn74 of *Np*HtrII is altered upon formation of the M-intermediate [103,104]. This alternation of the hydrogen bonding network is considered to be the origin of the weakened interaction between *Np*SRII and *Np*HtrII at the M-intermediate. Dr. Engelhard and coworkers reported that time-resolved electron paramagnetic resonance (EPR) and site-directed spin labeling (SDSL) methods revealed an outward tilting of helix-F of the isolated *Np*SRII during the M_1-to-M_2 process [105] (Fig. 8). Additionally, in the *Np*SRII/*Np*HtrII complex, a clockwise rotation of helix-TM2 of *Np*HtrII which is neighboring to helix-F of *Np*SRII was observed [88], and the degree of tilting of helix-F might be suppressed by the collision with helix-TM2 [88] (Fig. 8). A similar helix-TM2 rotation was observed in the crystallographic structure of the M (M_2) intermediate [106]. While the tilted helix-F recovers concomitantly with the recovery of the absorption change of *Np*SRII, helix-TM2 returns back to its original position 200 ms after the relaxation of the receptor [105]. A similar prolonged conformational change of *Np*HtrII after the recovery of the sensor part was observed in the change of its partial volume by transient grating measurements [107]. The delay of the recovery of the conformational change of *Np*HtrII with regard to *Np*SRII might enable the regulation of the transducer activity according to the cell's own physiological requirements. The dynamic helical movements of *Np*SRII and *Np*HtrII are considered to be one of the key processes for the signal transduction (Fig. 8).

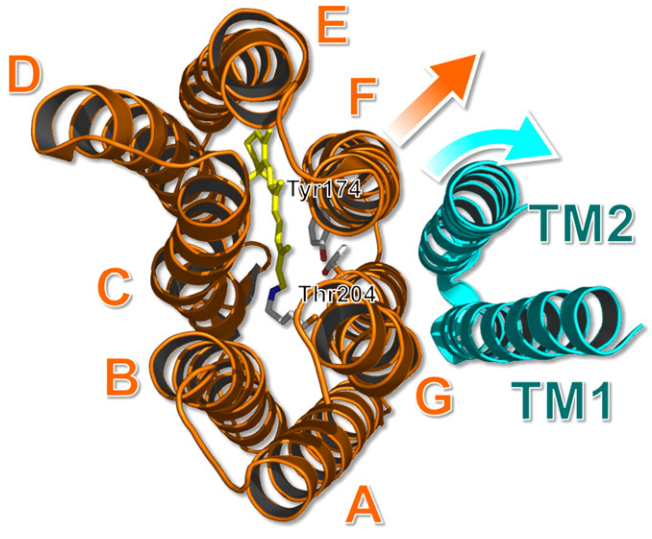

Fig. 8. Movement of the helices of *Np*SRII and *Np*HtrII observed in EPR measurements by using spin-labeled proteins. This view is from the cytoplasmic side [73,88].

Compared with the M-intermediate, the structural changes upon formation of the O-intermediate are less known. In 2008, we found that the *Np*SRII$_O$ minus *Np*SRII FTIR difference spectra of the O-decay accelerated mutants, SETC, were clearly different from those of the wild type, especially in the region of the amide-I (1680–1640 cm^{-1}) vibrations [108]. The bands at 1673 (+) and 1656 (−) cm^{-1} newly appear for SETC in the frequency region typical for the amide-I vibration of the α_{II}- and α_I-helices, respectively. The intensities of the band at 1673 (+) cm^{-1} of various O-decay accelerated mutants were well correlated with their O-decay half-times. Since the α_{II}-helix possesses a considerably distorted structure, the results imply that the distortion of the helix is required for a fast O-decay. Thus, we conclude that the lifetime of the O intermediate in *Np*SRII is regulated by a distorted α-helix.

3.5. Signal transfer mechanism in SRII-HtrII

As already mentioned, we succeeded in the identification of the residues participating in the structure and structural changes of *Np*SRII. We have then examined whether these residues are essential for the signaling by using the motility assay [109]. Unexpectedly, only the mutation on Thr204 or Tyr174 abolished the signal transduction, indicating that the other residues, Thr189 and Tyr199, and the E-F loop of *Np*SRII are not essential for the signaling. These two residues, Tyr174 and Thr204, are the first in *Np*SRII shown to be essential for phototaxis, and add biological significance to the previous observation that the hydrogen bond between them is greatly strengthened upon formation of the earliest *Np*SRII photointermediate (*Np*SRII$_K$) only when *Np*SRII is complexed with *Np*HtrII (Fig. 7B). Tyr174 is part of the retinal-binding site, and is conserved as Tyr185 in BR. Thr204 corresponds in position to Ala215 in BR, and is the principal component of a π-bulge on helix G present in both *Np*SRII and BR (Fig. 1B). To further confirm the importance of Thr204, we introduced A215T into the P200T/V210Y double mutant of BR which is able to interact with *Np*HtrII. The triple mutant of BR (BR-T) exhibits a slow photocycle and a lack of light-driven proton transport activity similar to *Np*SRII [110]. Interestingly, BR-T mediates phototaxis responses assessed as transient changes to light stimuli [110]. Furthermore, the A215T mutation in BR, even without the two mutations that introduce those residues which form hydrogen bonds with HtrII, was sufficient to mediate a very low but detectable phototaxis response. Recently, the crystal structure of the signal competent mutant of BR has been solved by Drs. Luecke and Spudich [111]. It showed that the introduced Thr residue is positioned nearly identically with respect to the retinal chromophore as in *Np*SRII. To investigate the structural changes of BR-T, we measured the FTIR spectra, and compared them with those of both BR and *Np*SRII [112]. The bands of the amide-I and C=N stretching vibration of BR-T were identical to those of the BR wild-type. In contrast, also characteristic aspects of *Np*SRII such as the hydrogen-out-of-plane (HOOP) modes of the retinal which represent the degrees of the distortion of the chromophore, the upshift of the O–H stretching vibration of Thr204 (Thr215 in BR-T) and the distorted α-helical structure were observed in BR-T [112]. These common features of *Np*SRII and BR-T

indicate that these factors should be important for the signal transduction. Actually, we found a positive correlation between the vibrational amplitudes of the C_{14} atom at 77 K and the efficiency of the physiological phototaxis response [100]. These observations strongly suggest that the steric constraint between the C_{14} group of the retinal and Thr204 of the protein (Fig. 7B) is prerequisite for the light-signal transduction of *Np*SRII. Thus, we concluded that Thr204 is important not only for the color tuning and the photocycle kinetics, but also for the negative phototaxis function (Fig. 5B).

Previously we applied FTIR spectroscopy to the active M intermediate in the absence and presence of *Np*HtrII [103]. The obtained difference FTIR spectra were surprisingly similar, notwithstanding the presence of *Np*HtrII. This result strongly suggests that the transducer activation in the *Np*SRII–*Np*HtrII system does not induce secondary structure alterations of *Np*HtrII itself. On the other hand, we found that the hydrogen bond of Asn74 in *Np*HtrII is strengthened in the M intermediate, presumably caused by change in its interaction with Tyr199 of *Np*SRII (Fig. 7). These facts provided evidence for a light signaling pathway from Lys205 (retinal) of the receptor to Asn74 of the transducer through Thr204 and Tyr199 (Fig. 7B). After that, we measured the temperature dependence of the M minus *Np*SRII spectra in the absence and presence of *Np*HtrII at 250–293 K [113]. Significant temperature dependence was observed for the amide-I vibrations of the helices only for the *Np*SRII/*Np*HtrII complex, in which the amplitude of the amide-I vibrations was reduced at room temperature. ^{13}C-labeling of *Np*SRII or *Np*HtrII revealed that such spectral changes in the bands of the helices originate from *Np*SRII and not *Np*HtrII. The temperature-dependent structural changes of the helices were diminished in the case of the complexes of *Np*SRII with the G83C or G83F mutant of *Np*HtrII, where Gly83 is believed to connect the transmembrane helix and the cytosolic linker region in a flexible kink near the membrane surface of *Np*HtrII, and its replacement by Cys or Phe abolishes the photosensory function [114]. The study provides direct experimental evidence that Gly83 plays an important structural role in the activation processes of the *Np*SRII/*Np*HtrII complex.

The importance of the salt bridge between the retinylidene Schiff base and its counterion aspartate for signal transduction was studied by several groups. Dr. Spudich et al. reported that a mutant of *Hs*SRII whose counterion aspartate 73 was replaced by Asn showed partial constitutive repellent signaling in its unphotolyzed state in the complex with *Hs*HtrII [115]. In contrast, the *Np*SRII D75N mutant (homologous to *Hs*SRII D73N) combined with *Np*HtrII showed an identical photo-response as wild-type *Np*SRII, and no dark reversing activity was observed [107]. These results of salt bridge breaking of *Hs*SRII/*Hs*HtrII and *Np*SRII/*Np*HtrII indicate differences in the signaling mechanism of these two systems. To confirm this hypothesis, Dr. Sasaki et al. studied the complexes between various counterion mutants of SRIIs and wild-type- or chimeric HtrIIs [116]. While the *Np*SRII D75Q mutant had an identical activity with the wild-type in complex with *Np*HtrII, the same mutant in complex with *Hs*HtrII was constitutively active. Furthermore, the *Np*SRII D75Q mutant in complex with the HtrII chimera of the N-terminal transmembrane (TM) domain of *Np*HtrII and the C-terminal cytoplasmic domain of *Hs*HtrII was shown to be of the null dark reversal phenotype. Thus, the type of the TM region of the HtrIIs determines the dark reversing activity when it is in complex with a *Np*SRII counterion mutant. From structural view point, *Np*SRII D75N mutant shows similar conformational changes like wild type *Np*SRII, indicating that the salt bridge is not a prerequisite for signal transfer (but certainly for proton transfer) [117].

On the basis of these results, and other findings, a model for the signal transduction by the *Np*SRII–*Np*HtrII system was proposed [33]; i) *trans-cis* photoisomerization of the retinal chromophore, ii) steric hindrance between C_{14}–H of the retinal and Thr204, iii) hydrogen bonding alteration between Thr204 and Tyr174, iv) F-helix outward tilting of *Np*SRII, v) TM-2 rotation of *Np*HtrII, vi) dissociation of the HAMP domain of *Np*HtrII from *Np*SRII, vii) structural changes in the Highly Conserved Domain (HCD), and viii) activation (phosphorylation) of CheA.

3.6. Evolutionary aspects of SRII

The phylogenic analysis strongly suggests that SRII evolved from BR [24,118] after gene duplication [119], and that SRI was generated by gene duplication from SRII (Fig. 1A). This is supported by the residual proton-pumping activities of *Hs*SRI and *Np*SRII isolated from their cognate transducers [36,75,120]. The phylogenic relationship between SRII and BR suggests the presence of common features in the mechanism of their functions of signal transduction and proton pumping. Accordingly, both of SRII and BR show the similar outward tilting of helix-F during their photocycles [73,121,122], and BR can be converted to a photo-phobic receptor by the mutation of only three residues [110] as described above. Interestingly, similar 6th-helix tilting on the activated state was observed for type-2 rhodopsin (bovine rhodopsin), a member of G protein-coupled receptors (GPCRs) [123,124]. In 2006, Dr. Oesterhelt and coworkers identified a new rhodopsin which is located at the phylogenetically intermediate position between BR and SRII in the genome of *Haloquadratum walsbyi* [125], and it was named middle rhodopsin (MR) (Fig. 1A) [24]. MR shares 41% and 35% amino acid sequence identity with BR and SRII, respectively, and has several important amino acids for the proton pump function, such as Asp85, Asp96, Asp212, and Glu204 in BR, as well as some for the signaling, such as Tyr174 and Thr204 in *Np*SRII (Fig. 1B). Although, the absorption of MR is in the blue-light region ($\lambda_{max} = 485$ nm) similar to SRII, it shows a faster M-decay similar to BR [24]. Wild-type MR does not mediate a phototaxis response, whereas a mutant of MR with two key hydrogen-bonding residues located at the interaction surface with the transducer protein *Np*HtrII (MR-A201T/M211Y) shows robust phototaxis responses similar to SRII [24]. This indicates that MR has the potential capability of SRII-like phototaxis signaling. These features imply that upon the molecular evolution from BR to SRII, at first, the color of the pigment was shifted to the blue-light region and the pumping function was lost in the BR → MR transition, then the signal transduction function was acquired in the MR → SRII transition through interaction with a transducer protein similar to chemoreceptors. Consequently, SRII-HtrII had to be generated to become a functional unit for a negative phototaxis sensor with some downstream proteins, the adaptor protein CheW and the kinase CheA. Interestingly, the retinal composition of MR is altered by illumination, shifting from all-*trans*- to 11-*cis*-retinal, suggesting the functional importance of the 11-*cis*- and/or all-*trans*-retinal chromophores [126]. This indicates that MR might also be a missing link in the evolution from type-1 (microbial) to type-2 retinal proteins (animal), because MR is the first microbial rhodopsin molecule discovered that has 11-*cis* retinal as a chromophore similar to type-2 proteins. It should be noted that the genes encoding the Che proteins and the proteins of the flagellar motor are missing in the genomic sequence of *H. walsbyi*. Thus, a novel signaling pathway would be required for MR to function as a photosensor in its native cells. Recently, we characterized the unique protein MR by using spectroscopic methods. Particularly, time-resolved FTIR spectroscopy revealed that the photoisomerization of the all-*trans* retinal in MR induces a large perturbation of a β-sheet structure in the hydrophilic part of MR, which is a unique conformational change not observed in either BR or SRII [127].

4. Molecular mechanism for the positive phototaxis initiated by SRI

4.1. A highly stable homolog from Salinibacter ruber

Compared to SRII, the signal relay mechanism of SRI is poorly characterized. Although the studies on *Hs*SRI gave us important information on both structural changes and function in action, the instability of *Hs*SRI in the detergent micelles, especially in the presence of light or the absence of NaCl, hampers the study of the detailed molecular mechanism of the signaling. In 2008, we characterized a new

SRI-like protein from the halophilic eubacterium *Salinibacter ruber* [128], which is also known to have xanthorhodopsin (XR) (Fig. 1A), a proton pump rhodopsin functioning with an auxiliary carotenoid antenna, salinixanthin, which transfers light energy to the retinal to increase its pumping efficiency [129]. In the genome of *S. ruber* [130], two genes coding SRI-like proteins were identified (SRU_2511 and SRU_2579). While SRU_2579 could not be expressed in *E. coli*, SRU_2511 was highly expressed and it was named *Sr*SRI (Fig. 1A) [128]. *Sr*SRI was a highly stable protein even in detergent without NaCl [131]. The interaction between the *Sr*SRI molecules is very strong, and it forms higher oligomers (ca. 150–200 molecules included) even in solubilized condition [132]. The absorption maximum of *Sr*SRI is located at 557 nm (Fig. 4), which is slightly shorter than that of *Hs*SRI (λ_{max} = 587 nm) [133] and similar to XR (λ_{max} = ~560 nm) [129]. This is reasonable because *Sr*SRI would function as a positive phototaxis sensor for XR. The retinal of *Sr*SRI is predominantly in its all-*trans* form (>90%) both in the dark and under light-illuminated conditions, which is similar to *Hs*SRI [128]. Furthermore, *Sr*SRI shows similar photocycle kinetics to those of *Hs*SRI, and the excitation of the M intermediate of *Sr*SRI generates an intermediate (P525) similar to *Hs*SRI [128] (Figs. 3A and 9). Thus, *Sr*SRI could act as a dual photosensor for positive phototaxis toward longer visible light and for a photophobic response to UV-radiation. On the other hand, the *pK*a of the counterion of *Sr*SRI is 4.3, and thus, much lower than that of *Hs*SRI (~7.2) [134]. Therefore, the deprotonated state is considered to be the physiologically functional state in the case of *Sr*SRI. In fact, *S. ruber* cells show both negative and positive phototaxis at neutral pH upon blue and green light illumination, respectively (unpublished data).

4.2. Chloride binding

Halophilic organisms including *H. salinarum, N. pharaonis* and *S. ruber* live in highly halophilic environments, suggesting the possibility of the effect(s) of salts on the functions of the retinal proteins. BR does not bind any chloride ion under physiological conditions, whereas HR binds a chloride ion (or chloride ions) inside the protein moiety (Fig. 10A) [19,58]. This is quite reasonable since HR works as a light-driven chloride ion pump. Some spectroscopic and structural studies clarified the binding position of the chloride ion as well as the local structure around the Schiff base in the ground state. The anion itself interacts with the proton of the protonated Schiff base (PSB) and the hydroxyl group of Ser115 in *Hs*HR (Ser130 in *Np*HR) (Fig. 10A). In the case of *Sr*SRI, its high stability enabled the measurement of absorption spectra at various salt concentrations. Upon Cl^- binding, the absorption maximum of *Sr*SRI is shifted from 542 to

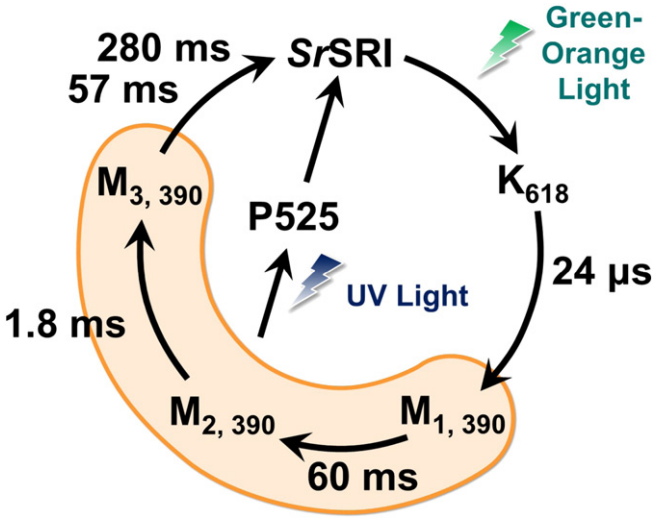

Fig. 9. Schematic diagram of the photocycle of *Sr*SRI with NaCl including the spectrally silent intermediates identified by the Transient Grating (TG) method.

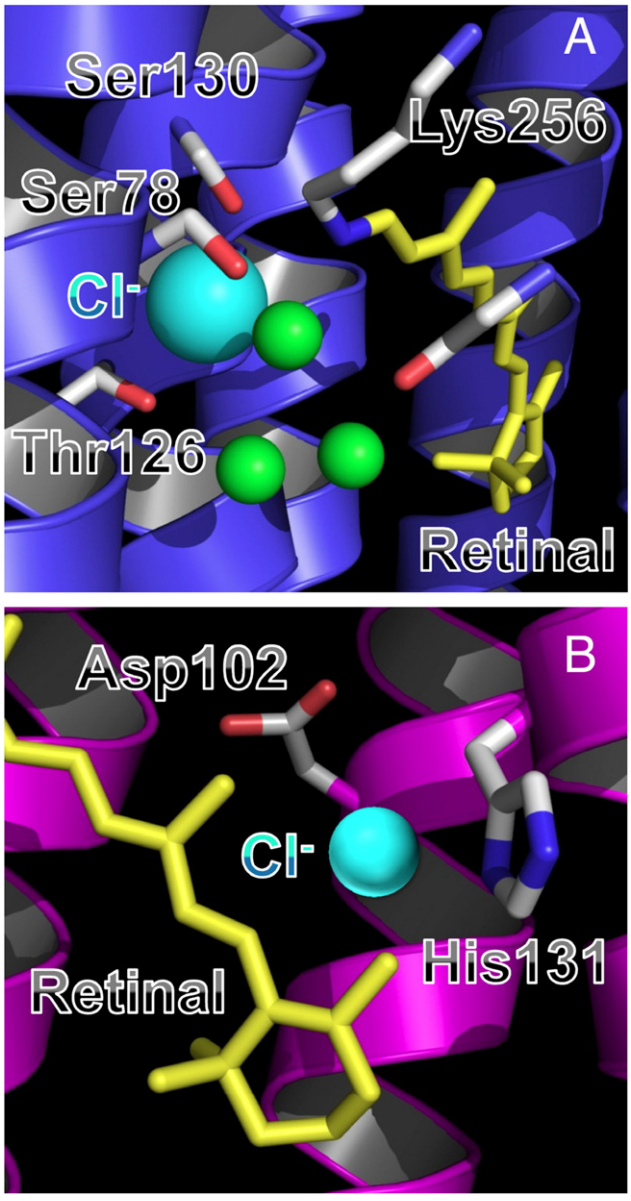

Fig. 10. Chloride binding site for *Np*HR (A) with water molecules (green) and the estimated putative Cl^- binding cavity for *Sr*SRI (B). The structure of *Sr*SRI was generated using the theoretical model of *Hs*SRI (Protein Data Bank ID: 1SR1).

556 nm with an affinity of 307 ± 56 mM. The binding of Cl^- to *Sr*SRI is much weaker than those of HRs (K_D = 10 [135] and 1 mM [136] for HR of *H. salinarum* and *N. pharaonis*, respectively). In addition to Cl^-, other anions (Br^-, I^- and NO_3^-) can bind to *Sr*SRI and their bindings are stronger than that of Cl^-, whereas no binding of F^- and SO_4^{2-} was observed [131]. These features are similar to the HRs. In contrast, the anion binding induces a spectral blue shift in the case of *Np*HR (without and with Cl^-, λ_{max} = 600 and 577 nm, respectively) but a spectral red shift [Δ = +14 nm] in the case of *Sr*SRI, which goes in the opposite direction. In addition, the chloride binding to *Sr*SRI does not alter the *pKa* of the counterion Asp72, indicating that the binding site is located near the polyene chain and/or the β-ionone ring. From mutational analysis, we estimated that the conserved residues among SRI-like proteins His131 and Asp102 located around the β-ionone ring are involved in the anion binding in *Sr*SRI (Fig. 10B) [131,137]. Thus, the different effects of the anion binding on the spectral tuning in *Sr*SRI and *Np*HR can be explained by the difference in binding site (Fig. 10). The Cl^- binding also affects the dynamics of *Sr*SRI. The M-decay rate of *Sr*SRI without NaCl (τ = 25 ms) was ~5-times faster

than that in the presence of NaCl ($\tau = 115$ ms), which is relatively close to that of BR ($\tau = 5$ ms) [131]. Thus, as expected, *Sr*SRI can be a key protein in the investigation of the functions of SRI at a molecular level.

4.3. Photochemical properties of SrSRI

Low-temperature FTIR studies on the K-formation of *Sr*SRI revealed that extended chromophore distortions take place in *Sr*SRI, similar to *Np*SRII and BR-T, whereas the distortion is localized at the Schiff base region in BR and HR [138]. It appears that the sensor and pump functions are distinguishable from such spectral features in the HOOP modes. On the other hand, the C_{14}-HOOP band at 864 cm^{-1} for *Np*SRII or 861 cm^{-1} for BR-T, respectively, which has been shown to be important for negative phototaxis, is absent in *Sr*SRI, suggesting that the changes of the C_{14}-H HOOP modes are specific features among sensors for negative phototaxis. This is reasonable because the counterpart of the C_{14} atom, Thr204 of *Np*SRII and Thr215 in BR-T, is not conserved in other microbial rhodopsins, including SRIs (Fig. 1B). In addition, the deprotonation of the residue Asp102, conserved among microbial retinal proteins, was observed upon formation of the M intermediate in the absence of Cl^- [137,139]. Furthermore, electrical chemical measurement with an indium tin oxide (ITO) electrode observed a proton uptake which occurs after the formation of the M intermediate in the absence of Cl^-. This delay from the formation of the M intermediate indicates that the multiple substates of M are present. In fact, transient grating method identified three such substates of M (M_1, M_2 and M_3) which have different partial molecular volumes [132], and the presence of these substates could represent the multiple proton transfer processes (Fig. 9). The enthalpy changes (ΔH) of each intermediate from the initial state are affected by the binding of Cl^-, and elevations of the ΔHs were observed for the K, M_1 and M_2 intermediates for the Cl^--bound form compared with the unbound form [132]. In addition, the mutant of Asp102 to glutamate (D102E) showed low stability compared with the wild-type, especially in the absence of Cl^-. This indicates that the Cl^--binding to the pocket which includes Asp102 contributes to the high stability of *Sr*SRI. Recently, we also found that an SRI homologue from the archaeon *Haloarcula vallismortis* (*Hv*SRI) exhibited similar alterations due to chloride ion binding [140]. Thus, the Cl^- binding is likely to be important for the function of the SRI protein family. It should be noted that in *Hv*SRI, five residues which are important for the phototaxis signaling of *Hs*SRI (H135, N165, H166, D201 and R215) are completely conserved, whereas they are not conserved in *Sr*SRI (Fig. 1B). Thus, comparative study on *Sr*SRI and *Hv*SRI are expected to reveal the differences in the molecular mechanism of the signal transduction between eubacterial and archaeal species.

The high stability of *Sr*SRI also enabled the design of multiple mutant proteins, which could be used in the study on the color tuning mechanism between SRI and SRII. *Sr*SRI ($\lambda_{max} = 557$ nm) has a 59 nm (2127 cm^{-1}) red-shifted visible absorption compared to *Np*SRII ($\lambda_{max} = 498$ nm) (Fig. 4). The difference in the λ_{max} between these proteins is generally considered to be caused by the differences of amino acid residues around the retinal. In a comprehensive mutational study of *Sr*SRI and *Np*SRII, the mutations of three residues in each protein (His131, Ala136 and Ala200 in *Sr*SRI which are substituted to Phe134, Tyr139 and Thr204 in *Np*SRII) caused large spectral shifts [141]. Especially, the triple mutant of *Sr*SRI with three residues of *Np*SRII type (H131F/A136Y/A200T) showed a $\lambda_{max} = 525$ nm which is in the middle between wild-type *Sr*SRI and *Np*SRII (Fig. 5A). Thus, the concerting effect of the substitution of three residues and the Cl^- binding to His131 (and Asp102) could be the main determinant for the color tuning between SRI and SRII (Fig. 5A). We also analyzed the color tuning mechanism between some BR-like proteins (archearhodopsin-3, AR3, *Hw*BR and MR) and SRII by using mutagenesis, and finally identified the residues involved in the spectral shift (unpublished). These results are summarized in Fig. 5A. Interestingly, the contributing residues (region) to the color of the proteins differ among rhodopsins, indicating that color tuning is achieved in each cognate protein, independently.

In the case of the archeal HtrI, its full-length expression in *E. coli* has not been achieved, and thus, the study on the interaction and the signal transduction between SRI and HtrI was difficult. The transducer of *S. ruber* (*Sr*HtrI), however, could be heterologously expressed as a fusion protein with *Sr*SRI in *E. coli* [142]. The formation of the complex with *Sr*HtrI affects the absorption spectrum of *Sr*SRI, and it shows a 13-nm red-shift compared with its unbound state. In addition, the pK_a of the counterion of the retinylidene Schiff base, Asp72, has been affected by the complex formation with *Sr*HtrI [$pKa = 4.3$ (without *Sr*HtrI) and 4.9 (with *Sr*HtrI)]. This indicates that the chromophore binding pocket of *Sr*SRI is affected by the binding of its cognate transducer. The success of the full-length expression of *Sr*HtrI is expected to enable the study on the signal transduction mechanism from SRI and HtrI to Che proteins in detail.

4.4. Differences between SRI and SRII

As described above, the SRI-HtrI and SRII-HtrII complexes transmit a light signal through their cytoplasmic sensory signaling system, inducing opposite effects (i.e., the inactivation or activation of the kinase CheA) (Fig. 2). To investigate the structure and structural changes around the Schiff base of *Sr*SRI, we measured the reactivity with a water-soluble reagent, azide. Studies of the reactivity with azide gave insight into the changes in the active M-intermediate. In the case of *Np*SRII, the *Np*HtrII-free *Np*SRII protein has a 4.6-fold larger reactivity with azide, compared to that of the complex with *Np*HtrII [143,144]. It has been reported that a proton uptake occurs during the $NpSRII_M$ decay, and that an electrogenic proton transport from the cytoplasmic to the extracellular space has been observed in the case of the *Np*HtrII-free *Np*SRII [75]. This has been interpreted as follows: during the presence or decay of $NpSRII_M$, a cytoplasmic (CP) channel opens, leading to an increase in the water accessibility of the Schiff base, which results in an increase in its reactivity with azide. However, once *Np*SRII associates with *Np*HtrII, the electrogenic proton transport stops. Furthermore, several reports on the structure of BR and its mutants revealed movement of the helices during the photocycle [122]. The conformational change is largely located at the cytoplasmic end of helices F and G [145,146]. These movements open a narrow water-accessible channel in the protein, enabling the transfer of a proton from an aspartate residue to the Schiff base. Similar movements of helices during the photocycle were suggested for *Np*SRII by several experiments, while the photoinduced outward tilting of helix F is hampered by *Np*HtrII (Fig. 8) [73,147]. Thus, the decrease in the reactivity of *Np*SRII with azide can be interpreted by the closure of the CP channel (Fig. 5B). In the case of the *Sr*HtrI-free *Sr*SRI, the reactivity with azide is more than 1000-fold smaller than that of the complex with *Sr*HtrI, which is opposite to the observation in *Np*SRII [137]. By drawing an analogy with SRII, an inward tilting of helix F of $SrSRI_M$-*Sr*HtrI might occur. We demonstrated that the frequency shifts of the amide-I and amide-A vibrations of the α-helix, upon formation of the M-intermediate, were opposite between *Sr*SRI and *Np*SRII (a downshift and an upshift were observed, respectively) by using FTIR spectroscopy [138]. This indicates that the M formation is accompanied by a weakening of the hydrogen bonds of the α-helix in *Sr*SRI, while the hydrogen bonds of the α-helix in *Np*SRII are strengthened. Thus, the change of reactivity with azide can be related to the FTIR results. Drs. Sineshchekov and Spudich revealed opposite conformations during the attractant and repellent signaling of the *Hs*SRI-*Hs*HtrI and *Np*SRII-*Np*HtrII complexes from changes in the Schiff base connectivity switch (inward/outward) [148]. This signaling behavior may be well described with a two-state model for receptor signaling, which is most extensively studied in the case of chemoreceptors [149,150]. In the unphotolyzed state, the SRI-HtrI and SRII-HtrII

complexes favor the kinase states ON and OFF, respectively, while in the M-intermediate, they change their preference to other kinase states. Furthermore, the dynamic properties of the F-helices of the SRI-HtrI and SRII-HtrII complexes in the M-intermediate are consistent with the "frozen dynamic" model of chemoreceptors, in which the kinase inactivating receptor is more dynamic than the kinase activating one [151].

It is likely that the binding of the chloride ion to SRI is important for its function in the phototaxis response by optimizing its absorption maximum and maintaining a slow photocycle. His131 of *Sr*SRI is located close to the β-ionone ring, as is Asp102 (Fig. 10B). Thus, the residues responsible for changes in the structure and structural changes in *Sr*SRI are concentrated around the β-ionone ring of the retinal chromphore (Fig. 11). In addition, FTIR studies indicated the existence of new water molecules in the presence of anions, as expected, as such water molecules would occupy sites inside the protein that may be energetically unfavorable, such as the mainly hydrophobic β-ionone ring region, close to which the ion binding site lies [139]. In contrast to this, mutations on Asn105 in *Np*SRII (Asp102 in *Sr*SRI) did not affect the absorption maximum or protein stability, indicating that the structure, and structural changes, around the β-ionone ring between *Sr*SRI and *Np*SRII are considerably different [139], which might be responsible for inducing the opposite signaling effects. In the case of *Np*SRII, the alteration in the hydrogen bonding between Thr204 and Tyr174, which are both located in the Schiff base region in *Np*SRII near the *Np*HtrII binding surface, is essential for the signaling (Fig. 11A). Thus, both the positive and the negative phototaxis may be regulated by the common all-*trans* retinal, only at a different position (Schiff base region for SRII and β-ionone ring region for SRI) (Fig. 11).

5. A sensory rhodopsin-like protein from the cyanobacterium *Anabaena*

Anabaena sensory rhodopsin (ASR) was the first eubacterial sensory rhodopsin-like protein, identified from the freshwater cyanobacterium *Anabaena* sp. PCC7120 (Fig. 1A) [152]. Previous studies revealed unique properties of ASR: (i) Hydrophilic nature in the cytoplasmic-side structure; the atomic-resolution structure of ASR obtained by X-ray crystallography revealed that numerous hydrophilic residues are located in the cytoplasmic (CP) half channel and connected by water molecules [153]. In other microbial retinal proteins, the CP channel is highly hydrophobic. This hydrophilic nature provides a hydrophilic connection from the retinal chromophore to the cytoplasmic surface. (ii) Unusual Schiff base proton transfer; in general, except for HR, a light-induced proton release from the protonated Schiff base to its counterion, usually an aspartate, commonly occurs in all known type-1 retinal proteins. However, in the case of ASR, the Schiff base counterion Asp75, which corresponds to Asp85 in BR (Fig. 1B), does not work as a primary proton acceptor during the photocycle. The cytoplasmic residue Asp217, which corresponds to Leu223 in BR, serves as the proton acceptor in the C-terminal truncated mutant ASR, however it does not in the full-length ASR [154,155]. Further studies are required for the understanding of the proton transfer pathway in ASR. (iii) Photochromism; It was confirmed by retinal isomer and spectroscopic analyses that two distinct all-*trans* and 13-*cis* forms of ASR exist in mixture in the dark state, which is different from the color discrimination mechanism of SRI. Each of them has different absorption maxima (550 nm for all-*trans* and 537 nm for 13-*cis* forms, respectively) and is interconverted by illumination with blue (480 nm) or orange (590 nm) light [156]. (iv) Soluble cytoplasmic transducer; ASR is encoded in an operon along with a second gene that encodes a small (~14 kDa) soluble protein, named ASR transducer (ASRT) [152,157]. This is quite different from the haloarchaeal phototaxis transducers, HtrI and HtrII, which are membrane-embedded proteins, which form a tight hetero-tetrameric assembly [89,158]. A previous study by isothermal titration calorimetry revealed that ASRT binds to ASR with a moderate binding affinity (K_d = 8 μM) in an ASRT:ASR stoichiometry of 4:1 in detergent solution [157].

Thus, the photochemical properties of ASR and the interaction between ASR and ASRT have been investigated, but their functional roles have been poorly understood. A possible physiological role was proposed by Dr. Spudich and coworkers that ASR is involved in the regulation of gene expression depending on light intensity and/or quality [153,159]. It is known that cyanobacteria exhibit chromatic adaptation, a mechanism in which cyanobacteria adjust the pigment composition of their photosynthetic light-harvesting complexes based on the color of available light. In cyanobacteria, orange light illumination induces the synthesis of allophycocyanin (phycocyanin), whereas blue-green light irradiation stimulates the synthesis of phycoerythrin (phycoerythrocyanin) [160]. It is assumed that two competitive photoreceptors are participated in such a color discriminative gene expression based on the chromatic adaptation. We investigated the role(s) of ASR and ASRT on the regulation of the gene expression in *E. coli*, which lacks photo-induced behaviors [161]. In this research, ASR was shown to regulate, as a gene repressor,

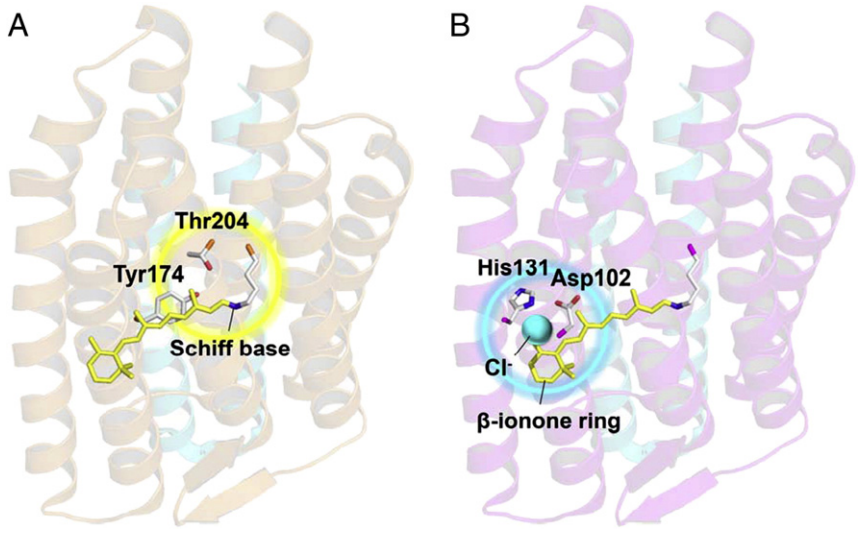

Fig. 11. Comparison between *Np*SRII (A) and *Sr*SRI (B). Functionally essential residues of *Np*SRII are concentrated around the Schiff base region of the retinal chromophore (yellow), while for *Sr*SRI, the residues involved in the maintenance of the structure and structural changes are mainly located around the β-ionone ring (blue).

the expression of the pigment protein phycocyanin. We proposed a model for the biological function of ASR and ASRT as follows [161]; (i) ASR having an all-*trans*-retinal chromophore in the dark represses the transcription of the chromatic adaptive gene cpcB (B subunit of phycocyanin) via the direct or indirect interaction with the promoter sequence of cpcB (PcpcB) through its C-terminal Arg residues, (ii) upon illumination, a structural change(s) of ASR is induced by the conversion of the retinal chromophore from all-*trans* to 13-*cis*, leading to the inhibition of the repression, (iii) ASRT may affect the expression via interaction with both ASR or PcpcB. According to these features, it was concluded that ASR serves as a photoreactive transcription factor and regulated the gene expression together with ASRT.

Other than the descriptions above, it has been recently revealed by solid-state NMR analysis that ASR forms a homo-trimeric assembly in lipid membrane [162]. As mentioned above, the haloarchaeal sensory rhodopsins form a tetrameric assembly composed of two units of SR-Htr hetero-dimeric complexes. Therefore, the homo-trimeric structure of ASR is unique among the sensory rhodopsin family proteins, and could be important for its physiological function in *Anabaena*. The functional regulation mechanism of ASR might be more similar to that of ion-pumping rhodopsins than to that of sensory rhodopsins, because the homo-trimeric structure is a common structural feature in the ion pumps from archaea to bacteria and contributes to their photoreaction [163–167]. Further studies are awaited to elucidate the functional regulation mechanism of the trimeric ASR and the interaction manner of the trimeric ASR and the tetrameric ASRT.

Acknowledgements

We wish to thank many collaborators, especially Drs. Louisa Reissig, Yuji Furutani, Masayuki Iwamoto, Kazumi Shimono, Naoki Kamo, John Spudich and Hideki Kandori. Our original publications were supported by a Grant-in-Aid from the Japanese Ministry of Education, Science, Technology, Sports and Cultures.

References

[1] J.L. Spudich, C.S. Yang, K.-H. Jung, E.N. Spudich, Retinylidene proteins: structures and functions from archaea to humans, Annu. Rev. Cell Dev. Biol. 16 (2000) 365–392.
[2] J.L. Spudich, K.-H. Jung, Microbial rhodopsin: Phylogenetic and functional diversity, Handbook of Photosensory Receptors, 2005, pp. 1–23.
[3] D. Oesterhelt, W. Stoeckenius, Rhodopsin-like protein from the purple membrane of *Halobacterium halobium*, Nat. New Biol. 233 (1971) 149–152.
[4] H. Luecke, B. Schobert, H.T. Richter, J.P. Cartailler, J.K. Lanyi, Structure of bacteriorhodopsin at 1.55 A resolution, J. Mol. Biol. 291 (1999) 899–911.
[5] M. Shibata, T. Tanimoto, H. Kandori, Water molecules in the schiff base region of bacteriorhodopsin, J. Am. Chem. Soc. 125 (2003) 13312–13313.
[6] Y. Mukohata, K. Ihara, T. Tamura, Y. Sugiyama, Halobacterial rhodopsins, J. Biochem. 125 (1999) 649–657.
[7] J.K. Lanyi, Bacteriorhodopsin, Annu. Rev. Physiol. 66 (2004) 665–688.
[8] O. Béjà, L. Aravind, E.V. Koonin, M.T. Suzuki, A. Hadd, L.P. Nguyen, S.B. Jovanovich, C.M. Gates, R.A. Feldman, J.L. Spudich, E.N. Spudich, E.F. DeLong, Bacterial rhodopsin: evidence for a new type of phototrophy in the sea, Science 289 (2000) 1902–1906.
[9] S.A. Waschuk, A.G. Bezerra Jr., L. Shi, L.S. Brown, *Leptosphaeria rhodopsin*: bacteriorhodopsin-like proton pump from a eukaryote, Proc. Natl. Acad. Sci. U. S. A. 102 (2005) 6879–6883.
[10] S.P. Tsunoda, D. Ewers, S. Gazzarrini, A. Moroni, D. Gradmann, P. Hegemann, H^+-pumping rhodopsin from the marine alga *Acetabllaria*, Biophys. J. 91 (2006) 1471–1479.
[11] S.P. Balashov, E.S. Imasheva, V.A. Boichenko, J. Anton, J.M. Wang, J.K. Lanyi, Xanthorhodopsin: a proton pump with a light-harvesting carotenoid antenna, Science 309 (2005) 2061–2064.
[12] M.R. Miranda, A.R. Choi, L. Shi, A.G. Bezerra Jr., K.-H. Jung, L.S. Brown, The photocycle and proton translocation pathway in a cyanobacterial ion-pumping rhodopsin, Biophys. J. 96 (2009) 1471–1481.
[13] S.P. Balashov, L.E. Petrovskaya, E.P. Lukashev, E.S. Imasheva, A.K. Dioumaev, J.M. Wang, S.V. Sychev, D.A. Dolgikh, A.B. Rubin, M.P. Kirpichnikov, J.K. Lanyi, Aspartate-histidine interaction in the retinal Schiff base counterion of the light-driven proton pump of *Exiguobacterium sibiricum*, Biochemistry 51 (2012) 5748–5762.
[14] L.E. Petrovskaya, E.P. Lukashev, V.V. Chupin, S.V. Sychev, E.N. Lyukmanova, E.A. Kryukova, R.H. Ziganshin, E.V. Spirina, E.M. Rivkina, R.A. Khatypov, L.G. Erokhina, D.A. Gilichinsky, V.A. Shuvalov, M.P. Kirpichnikov, Predicted bacteriorhodopsin from *Exiguobacterium sibiricum* is a functional proton pump, FEBS Lett. 584 (2010) 4193–4196.
[15] K. Inoue, H. Ono, R. Abe-Yoshizumi, S. Yoshizawa, H. Ito, K. Kogure, H. Kandori, A light-driven sodium ion pump in marine bacteria, Nat. Commun. 4 (2013) 1678.
[16] A. Matsuno-Yagi, Y. Mukohata, Two possible roles of bacteriorhodopsin; a comparative study of strains of *Halobacterium halobium* differing in pigmentation, Biochem. Biophys. Res. Commun. 78 (1977) 237–243.
[17] B. Schobert, J.K. Lanyi, Halorhodopsin is a light-driven chloride pump, J. Biol. Chem. 257 (1982) 10306–10313.
[18] G. Varo, Analogies between halorhodopsin and bacteriorhodopsin, Biochim. Biophys. Acta 1460 (2000) 220–229.
[19] T. Kouyama, S. Kanada, Y. Takeguchi, A. Narusawa, M. Murakami, K. Ihara, Crystal structure of the light-driven chloride pump halorhodopsin from *Natronomonas pharaonis*, J. Mol. Biol. 396 (2010) 564–579.
[20] J. Sasaki, L.S. Brown, Y.S. Chon, H. Kandori, A. Maeda, R. Needleman, J.K. Lanyi, Conversion of bacteriorhodopsin into a chloride ion pump, Science 269 (1995) 73–75.
[21] T. Kouyama, M. Murakami, Structural divergence and functional versatility of the rhodopsin superfamily, Photochem. Photobiol. Sci. 9 (2010) 1458–1465.
[22] A. Nakatsuma, T. Yamashita, K. Sasaki, A. Kawanabe, K. Inoue, Y. Furutani, Y. Shichida, H. Kandori, Chimeric microbial rhodopsins containing the third cytoplasmic loop of bovine rhodopsin, Biophys. J. 100 (2011) 1874–1882.
[23] A.H. Geiser, M.K. Sievert, L.W. Guo, J.E. Grant, M.P. Krebs, D. Fotiadis, A. Engel, A.E. Ruoho, Bacteriorhodopsin chimeras containing the third cytoplasmic loop of bovine rhodopsin activate transducin for GTP/GDP exchange, Protein Sci. 15 (2006) 1679–1690.
[24] Y. Sudo, K. Ihara, S. Kobayashi, D. Suzuki, H. Irieda, T. Kikukawa, H. Kandori, M. Homma, A microbial rhodopsin with a unique retinal composition shows both sensory rhodopsin II and bacteriorhodopsin-like properties, J. Biol. Chem. 286 (2011) 5967–5976.
[25] M. Koyanagi, E. Takada, T. Nagata, H. Tsukamoto, A. Terakita, Homologs of vertebrate Opn3 potentially serve as a light sensor in nonphotoreceptive tissue, Proc. Natl. Acad. Sci. U. S. A. 110 (2013) 4998–5003.
[26] L. Shen, C. Chen, H. Zheng, L. Jin, The evolutionary relationship between microbial rhodopsins and metazoan rhodopsins, ScientificWorldJournal 2013 (2013) 435651.
[27] R.A. Bogomolni, J.L. Spudich, Identification of a third rhodopsin-like pigment in phototactic *Halobacterium halobium*, Proc. Natl. Acad. Sci. U. S. A. 79 (1982) 6250–6254.
[28] T. Takahashi, H. Tomioka, N. Kamo, Y. Kobatake, A photosystem other than PS370 also mediates the negative phototaxis of *Halobacterium halobium*, FEMS Microbiol. Lett. 28 (1985) 161–164.
[29] D. Suzuki, H. Irieda, M. Homma, I. Kawagishi, Y. Sudo, Phototactic and chemotactic signal transduction by transmembrane receptors and transducers in microorganisms, Sensors (Basel) 10 (2010) 4010–4039.
[30] W.D. Hoff, K.H. Jung, J.L. Spudich, Molecular mechanism of photosignaling by archaeal sensory rhodopsins, Annu. Rev. Biophys. Biomol. Struct. 26 (1997) 223–258.
[31] X.N. Zhang, J. Zhu, J.L. Spudich, The specificity of interaction of archaeal transducers with their cognate sensory rhodopsins is determined by their transmembrane helices, Proc. Natl. Acad. Sci. U. S. A. 96 (1999) 857–862.
[32] J.J. Falke, R.B. Bass, S.L. Butler, S.A. Chervitz, M.A. Danielson, The two-component signaling pathway of bacterial chemotaxis: a molecular view of signal transduction by receptors, kinases, and adaptation enzymes, Annu. Rev. Cell Dev. Biol. 13 (1997) 457–512.
[33] J.P. Armitage, Bacterial tactic responses, Adv. Microb. Physiol. 41 (1999) 229–289.
[34] M.D. Baker, P.M. Wolanin, J.B. Stock, Signal transduction in bacterial chemotaxis, Bioessays 28 (2006) 9–22.
[35] J.L. Spudich, R.A. Bogomolni, Mechanism of colour discrimination by a bacterial sensory rhodopsin, Nature 312 (1984) 509–513.
[36] R.A. Bogomolni, W. Stoeckenius, I. Szundi, E. Perozo, K.D. Olson, J.L. Spudich, Removal of transducer HtrI allows electrogenic proton translocation by sensory rhodopsin I, Proc. Natl. Acad. Sci. U. S. A. 91 (1994) 10188–10192.
[37] K.D. Olson, J.L. Spudich, Removal of the transducer protein from sensory rhodopsin I exposes sites of proton release and uptake during the receptor photocycle, Biophys. J. 65 (1993) 2578–2585.
[38] T. Takahashi, Y. Mochizuki, N. Kamo, Y. Kobatake, Evidence that the long-lifetime photointermediate of s-rhodopsin is a receptor for negative phototaxis in *Halobacterium halobium*, Biochem. Biophys. Res. Commun. 127 (1985) 99–105.
[39] H. Tomioka, T. Takahashi, N. Kamo, Y. Kobatake, Flash spectrophotometric identification of a fourth rhodopsin-like pigment in *Halobacterium halobium*, Biochem. Biophys. Res. Commun. 139 (1986) 389–395.
[40] E.N. Spudich, S.A. Sundberg, D. Manor, J.L. Spudich, Properties of a second sensory receptor protein in *Halobacterium halobium* phototaxis, Proteins 1 (1986) 239–246.
[41] Y. Shichida, Y. Imamoto, T. Yoshizawa, T. Takahashi, H. Tomioka, N. Kamo, Y. Kobatake, Low-temperature spectrophotometry of phoborhodopsin, FEBS Lett. 236 (1988) 333–336.
[42] Y. Imamoto, Y. Shichida, T. Yoshizawa, H. Tomioka, T. Takahashi, K. Fujikawa, N. Kamo, Y. Kobatake, Photoreaction cycle of phoborhodopsin studied by low-temperature spectrophotometry, Biochemistry 30 (1991) 7416–7424.
[43] B. Scharf, B. Pevec, B. Hess, M. Engelhard, Biochemical and photochemical properties of the photophobic receptors from *Halobacterium halobium* and *Natronobacterium pharaonis*, Eur. J. Biochem. 206 (1992) 359–366.

[44] J. Sasaki, J.L. Spudich, The transducer protein HtrII modulates the lifetimes of sensory rhodopsin II photointermediates, Biophys. J. 75 (1998) 2435–2440.
[45] J. Sasaki, J.L. Spudich, Proton circulation during the photocycle of sensory rhodopsin II, Biophys. J. 77 (1999) 2145–2152.
[46] J. Sasaki, J.L. Spudich, Proton transport by sensory rhodopsins and its modulation by transducer-binding, Biochim. Biophys. Acta 1460 (2000) 230–239.
[47] B. Yan, T. Takahashi, R. Johnson, J.L. Spudich, Identification of signaling states of a sensory receptor by modulation of lifetimes of stimulus-induced conformations: the case of sensory rhodopsin II, Biochemistry 30 (1991) 10686–10692.
[48] Y. Nakao, T. Kikukawa, K. Shimono, J. Tamogami, N. Kimitsuki, T. Nara, M. Unno, K. Ihara, N. Kamo, Photochemistry of a putative new class of sensory rhodopsin (SRIII) coded by xop2 of *Haloarcular marismortui*, J. Photochem. Photobiol. B 102 (2011) 45–54.
[49] J. Hirayama, Y. Imamoto, Y. Shichida, N. Kamo, H. Tomioka, T. Yoshizawa, Photocycle of phoborhodopsin from haloalkaliphilic bacterium (*Natronobacterium pharaonis*) studied by low-temperature spectrophotometry, Biochemistry 31 (1992) 2093–2098.
[50] B. Lüttenberg, E.K. Wolff, M. Engelhard, Heterologous coexpression of the blue light receptor psRII and its transducer pHtrII from *Natronobacterium pharaonis* in the *Halobacterium salinarium* strain Pho81/w restores negative phototaxis, FEBS Lett. 426 (1998) 117–120.
[51] K. Shimono, M. Iwamoto, M. Sumi, N. Kamo, Functional expression of pharaonis phoborhodopsin in *Escherichia coli*, FEBS Lett. 420 (1997) 54–56.
[52] Y. Sudo, M. Iwamoto, K. Shimono, N. Kamo, Pharaonis phoborhodopsin binds to its cognate truncated transducer even in the presence of a detergent with a 1:1 stoichiometry, Photochem. Photobiol. 74 (2001) 489–494.
[53] N. Mennes, J.P. Klare, I. Chizhov, R. Seidel, R. Schlesinger, M. Engelhard, Expression of the halobacterial transducer protein HtrII from *Natronomonas pharaonis* in *Escherichia coli*, FEBS Lett. 581 (2007) 1487–1494.
[54] Y. Sudo, M. Yamabi, M. Iwamoto, K. Shimono, N. Kamo, Interaction of *Natronobacterium pharaonis* phoborhodopsin (sensory rhodopsin II) with its cognate transducer probed by increase in the thermal stability, Photochem. Photobiol. 78 (2003) 511–516.
[55] Y. Ikeura, K. Shimono, M. Iwamoto, Y. Sudo, N. Kamo, Arg-72 of *pharaonis* phoborhodopsin (sensory rhodopsin II) is important for the maintenance of the protein structure in the solubilized states, Photochem. Photobiol. 77 (2003) 96–100.
[56] H. Luecke, B. Schobert, J.K. Lanyi, E.N. Spudich, J.L. Spudich, Crystal structure of sensory rhodopsin II at 2.4 angstroms: insights into color tuning and transducer interaction, Science 293 (2001) 1499–1503.
[57] A. Royant, P. Nollert, K. Edman, R. Neutze, E.M. Landau, E. Pebay-Peyroula, J. Navarro, X-ray structure of sensory rhodopsin II at 2.1-A resolution, Proc. Natl. Acad. Sci. U. S. A. 98 (2001) 10131–10136.
[58] M. Kolbe, H. Besir, L.O. Essen, D. Oesterhelt, Structure of the light-driven chloride pump halorhodopsin at 1.8 A resolution, Science 288 (2000) 1390–1396.
[59] Y. Imamoto, Y. Shichida, J. Hirayama, H. Tomioka, N. Kamo, T. Yoshizawa, Chromophore configuration of *pharaonis* phoborhodopsin and its isomerization on photon absorption, Biochemistry 31 (1992) 2523–2528.
[60] J.K. Lanyi, V. Vodyanoy, Flash spectroscopic studies of the kinetics of the halorhodopsin photocycle, Biochemistry 25 (1986) 1465–1470.
[61] J. Hirayama, Y. Imamoto, Y. Shichida, T. Yoshizawa, A.E. Asato, R.S. Liu, N. Kamo, Shape of the chromophore binding site in *pharaonis* phoborhodopsin from a study using retinal analogs, Photochem. Photobiol. 60 (1994) 388–393.
[62] T. Takahashi, B. Yan, P. Mazur, F. Derguini, K. Nakanishi, J.L. Spudich, Color regulation in the archaebacterial phototaxis receptor phoborhodopsin (sensory rhodopsin II), Biochemistry 29 (1990) 8467–8474.
[63] S. Hayashi, E. Tajkhorshid, E. Pebay-Peyroula, A. Royant, E.M. Landau, J. Navarro, K. Schulten, Structural determinants of spectral tuning in retinal proteins-bacteriorhodopsin vs sensory rhodopsin II, J. Phys. Chem. B 105 (2001) 10124–10131.
[64] L. Ren, C.H. Martin, K.J. Wise, N.B. Gillespie, H. Luecke, J.K. Lanyi, J.L. Spudich, R.R. Birge, Molecular mechanism of spectral tuning in sensory rhodopsin II, Biochemistry 40 (2001) 13906–13914.
[65] K. Shimono, Y. Ikeura, Y. Sudo, M. Iwamoto, N. Kamo, Environment around the chromophore in *pharaonis* phoborhodopsin: mutation analysis of the retinal binding site, Biochim. Biophys. Acta 1515 (2001) 92–100.
[66] K. Shimono, T. Hayashi, Y. Ikeura, Y. Sudo, M. Iwamoto, N. Kamo, Importance of the broad regional interaction for spectral tuning in *Natronobacterium pharaonis* phoborhodopsin (sensory rhodopsin II), J. Biol. Chem. 278 (2003) 23882–23889.
[67] I. Lutz, A. Sieg, A.A. Wegener, M. Engelhard, I. Boche, M. Otsuka, D. Oesterhelt, J. Wachtveitl, W. Zinth, Primary reactions of sensory rhodopsins, Proc. Natl. Acad. Sci. U. S. A. 98 (2001) 962–967.
[68] M. Mizuno, Y. Sudo, M. Homma, Y. Mizutani, Direct observation of the structural change of Tyr174 in the primary reaction of sensory rhodopsin II, Biochemistry 50 (2011) 3170–3180.
[69] S.J. Doig, P.J. Reid, R.A. Mathies, Picosecond time-resolved resonance raman spectroscopy of bacteriorhodopdn's J, K, and KL Intermediates, J. Phys. Chem. 95 (1991) 6372–6379.
[70] R. Diller, R. Jakober, C. Schumann, F. Peters, J.P. Klare, M. Engelhard, The *trans-cis* isomerization reaction dynamics in sensory rhodopsin II by femtosecond time-resolved midinfrared spectroscopy: chromophore and protein dynamics, Biopolymers 82 (2006) 358–362.
[71] I. Chizhov, G. Schmies, R. Seidel, J.R. Sydor, B. Luttenberg, M. Engelhard, The photophobic receptor from *Natronobacterium pharaonis*: temperature and pH dependencies of the photocycle of sensory rhodopsin II, Biophys. J. 75 (1998) 999–1009.
[72] K. Inoue, J. Sasaki, M. Morisaki, F. Tokunaga, M. Terazima, Time-resolved detection of sensory rhodopsin II-transducer interaction, Biophys. J. 87 (2004) 2587–2597.
[73] A.A. Wegener, I. Chizhov, M. Engelhard, H.J. Steinhoff, Time-resolved detection of transient movement of helix F in spin-labelled *pharaonis* sensory rhodopsin II, J. Mol. Biol. 301 (2000) 881–891.
[74] Y. Imamoto, Y. Shichida, J. Hirayama, H. Tomioka, N. Kamo, S. Yoshizawa, Nanosecond laser photolysis of phoborhodopsin: from *Natronobacterium pharaonis* appearance of KL and L intermediates in the photocycle at room temperature, Photochem. Photobiol. 56 (1992) 1129–1134.
[75] Y. Sudo, M. Iwamoto, K. Shimono, M. Sumi, N. Kamo, Photo-induced proton transport of *pharaonis* phoborhodopsin (sensory rhodopsin II) is ceased by association with the transducer, Biophys. J. 80 (2001) 916–922.
[76] Y. Furutani, M. Iwamoto, K. Shimono, A. Wada, M. Ito, N. Kamo, H. Kandori, FTIR spectroscopy of the O photointermediate in *pharaonis* phoborhodopsin, Biochemistry 43 (2004) 5204–5212.
[77] J.K. Lanyi, Shuffling protons in bacteriorhodopsin: long-distance coupling between the pKas of two carboxylic groups, Biophys. J. 71 (1996) 541–543.
[78] J. Tittor, C. Soell, D. Oesterhelt, H.J. Butt, E. Bamberg, A defective proton pump, point-mutated bacteriorhodopsin Asp96–Asn is fully reactivated by azide, EMBO J. 8 (1989) 3477–3482.
[79] K. Takao, T. Kikukawa, T. Araiso, N. Kamo, Azide accelerates the decay of M-intermediate of *pharaonis* phoborhodopsin, Biophys. Chem. 73 (1998) 145–153.
[80] M. Iwamoto, K. Shimono, M. Sumi, N. Kamo, Positioning proton-donating residues to the Schiff-base accelerates the M-decay of *pharaonis* phoborhodopsin expressed in *Escherichia coli*, Biophys. Chem. 79 (1999) 187–192.
[81] N. Kamo, K. Shimono, M. Iwamoto, Y. Sudo, Photochemistry and photoinduced proton-transfer by pharaonis phoborhodopsin, Biochemistry (Mosc) 66 (2001) 1277–1282.
[82] R. Seidel, B. Scharf, M. Gautel, K. Kleine, D. Oesterhelt, M. Engelhard, The primary structure of sensory rhodopsin II: a member of an additional retinal protein subgroup is coexpressed with its transducer, the halobacterial transducer of rhodopsin II, Proc. Natl. Acad. Sci. U. S. A. 92 (1995) 3036–3040.
[83] J.P. Klare, G. Schmies, I. Chizhov, K. Shimono, N. Kamo, M. Engelhard, Probing the proton channel and the retinal binding site of *Natronobacterium pharaonis* sensory rhodopsin II, Biophys. J. 82 (2002) 2156–2164.
[84] M. Iwamoto, Y. Sudo, K. Shimono, T. Araiso, N. Kamo, Correlation of the O-intermediate rate with the pKa of Asp-75 in the dark, the counterion of the Schiff base of *pharaonis* phoborhodopsin (sensory rhodopsin II), Biophys. J. 88 (2005) 1215–1223.
[85] J.P. Klare, E. Bordignon, M. Doebber, J. Fitter, J. Kriegsmann, I. Chizhov, H.J. Steinhoff, M. Engelhard, Effects of solubilization on the structure and function of the sensory rhodopsin II/transducer complex, J. Mol. Biol. 356 (2006) 1207–1221.
[86] M. Hein, A.A. Wegener, M. Engelhard, F. Siebert, Time-resolved FTIR studies of sensory rhodopsin II (NpSRII) from *Natronobacterium pharaonis*: implications for proton transport and receptor activation, Biophys. J. 84 (2003) 1208–1217.
[87] S. Hippler-Mreyen, J.P. Klare, A.A. Wegener, R. Seidel, C. Herrmann, G. Schmies, G. Nagel, E. Bamberg, M. Engelhard, Probing the sensory rhodopsin II binding domain of its cognate transducer by calorimetry and electrophysiology, J. Mol. Biol. 330 (2003) 1203–1213.
[88] A.A. Wegener, J.P. Klare, M. Engelhard, H.J. Steinhoff, Structural insights into the early steps of receptor-transducer signal transfer in archaeal phototaxis, EMBO J. 20 (2001) 5312–5319.
[89] V.I. Gordeliy, J. Labahn, R. Moukhametzianov, R. Efremov, J. Granzin, R. Schlesinger, G. Buldt, T. Savopol, A.J. Scheidig, J.P. Klare, M. Engelhard, Molecular basis of transmembrane signalling by sensory rhodopsin II-transducer complex, Nature 419 (2002) 484–487.
[90] Y. Sudo, M. Iwamoto, K. Shimono, N. Kamo, Association between a photointermediate of a M-lacking mutant D75N of *pharaonis* phoborhodopsin and its cognate transducer, J. Photochem. Photobiol. B 67 (2002) 171–176.
[91] Y. Sudo, M. Iwamoto, K. Shimono, N. Kamo, Tyr-199 and charged residues of *pharaonis* Phoborhodopsin are important for the interaction with its transducer, Biophys. J. 83 (2002) 427–432.
[92] Y. Sudo, M. Yamabi, S. Kato, C. Hasegawa, M. Iwamoto, K. Shimono, N. Kamo, Importance of specific hydrogen bonds of archaeal rhodopsins for the binding to the transducer protein, J. Mol. Biol. 357 (2006) 1274–1282.
[93] Y. Sudo, H. Okuda, M. Yamabi, Y. Fukuzaki, M. Mishima, N. Kamo, C. Kojima, Linker region of a halobacterial transducer protein interacts directly with its sensor retinal protein, Biochemistry 44 (2005) 6144–6152.
[94] Y. Sudo, M. Iwamoto, K. Shimono, N. Kamo, Role of charged residues of *pharaonis* phoborhodopsin (sensory rhodopsin II) in its interaction with the transducer protein, Biochemistry 43 (2004) 13748–13754.
[95] Y. Kitade, Y. Furutani, N. Kamo, H. Kandori, Proton release group of *pharaonis* phoborhodopsin revealed by ATR-FTIR spectroscopy, Biochemistry 48 (2009) 1595–1603.
[96] H. Kandori, K. Shimono, Y. Sudo, M. Iwamoto, Y. Shichida, N. Kamo, Structural changes of pharaonis phoborhodopsin upon photoisomerization of the retinal chromophore: infrared spectral comparison with bacteriorhodopsin, Biochemistry 40 (2001) 9238–9246.
[97] Y. Furutani, Y. Sudo, N. Kamo, H. Kandori, FTIR spectroscopy of the complex between *pharaonis* phoborhodopsin and its transducer protein, Biochemistry 42 (2003) 4837–4842.
[98] Y. Sudo, Y. Furutani, K. Shimono, N. Kamo, H. Kandori, Hydrogen bonding alteration of Thr-204 in the complex between *pharaonis* phoborhodopsin and its transducer protein, Biochemistry 42 (2003) 14166–14172.
[99] Y. Sudo, Y. Furutani, A. Wada, M. Ito, N. Kamo, H. Kandori, Steric constraint in the primary photoproduct of an archaeal rhodopsin from regiospecific perturbation of C-D stretching vibration of the retinyl chromophore, J. Am. Chem. Soc. 127 (2005) 16036–16037.

[100] M. Ito, Y. Sudo, Y. Furutani, T. Okitsu, A. Wada, M. Homma, J.L. Spudich, H. Kandori, Steric constraint in the primary photoproduct of sensory rhodopsin II is a prerequisite for light-signal transfer to HtrII, Biochemistry 47 (2008) 6208–6215.
[101] Y. Sudo, H. Kandori, N. Kamo, Molecular mechanism of protein-protein interaction of *pharaonis* phoborhodopsin/transducer and photo-signal transfer reaction by the complex, Recent Res. Dev. Biophys. 3 (2004) 1–16.
[102] Y. Sudo, T. Nishihori, M. Iwamoto, K. Shimono, C. Kojima, N. Kamo, A long-lived M-like state of phoborhodopsin that mimics the active state, Biophys. J. 95 (2008) 753–760.
[103] Y. Furutani, K. Kamada, Y. Sudo, K. Shimono, N. Kamo, H. Kandori, Structural changes of the complex between *pharaonis* phoborhodopsin and its cognate transducer upon formation of the M photointermediate, Biochemistry 44 (2005) 2909–2915.
[104] V.B. Bergo, E.N. Spudich, K.J. Rothschild, J.L. Spudich, Photoactivation perturbs the membrane-embedded contacts between sensory rhodopsin II and its transducer, J. Biol. Chem. 280 (2005) 28365–28369.
[105] J.P. Klare, V.I. Gordeliy, J. Labahn, G. Buldt, H.J. Steinhoff, M. Engelhard, The archaeal sensory rhodopsin II/transducer complex: a model for transmembrane signal transfer, FEBS Lett. 564 (2004) 219–224.
[106] R. Moukhametzianov, J.P. Klare, R. Efremov, C. Baeken, A. Goppner, J. Labahn, M. Engelhard, G. Buldt, V.I. Gordeliy, Development of the signal in sensory rhodopsin and its transfer to the cognate transducer, Nature 440 (2006) 115–119.
[107] K. Inoue, J. Sasaki, J.L. Spudich, M. Terazima, Laser-induced transient grating analysis of dynamics of interaction between sensory rhodopsin II D75N and the HtrII transducer, Biophys. J. 92 (2007) 2028–2040.
[108] Y. Sudo, Y. Furutani, M. Iwamoto, N. Kamo, H. Kandori, Structural changes in the O-decay accelerated mutants of *pharaonis* phoborhodopsin, Biochemistry 47 (2008) 2866–2874.
[109] Y. Sudo, Y. Furutani, H. Kandori, J.L. Spudich, Functional importance of the interhelical hydrogen bond between Thr204 and Tyr174 of sensory rhodopsin II and its alteration during the signaling process, J. Biol. Chem. 281 (2006) 34239–34245.
[110] Y. Sudo, J.L. Spudich, Three strategically placed hydrogen-bonding residues convert a proton pump into a sensory receptor, Proc. Natl. Acad. Sci. U. S. A. 103 (2006) 16129–16134.
[111] E.N. Spudich, G. Ozorowski, E.V. Schow, D.J. Tobias, J.L. Spudich, H. Luecke, A transporter converted into a sensor, a phototaxis signaling mutant of bacteriorhodopsin at 3.0 A, J. Mol. Biol. 415 (2012) 455–463.
[112] Y. Sudo, Y. Furutani, J.L. Spudich, H. Kandori, Early photocycle structural changes in a bacteriorhodopsin mutant engineered to transmit photosensory signals, J. Biol. Chem. 282 (2007) 15550–15558.
[113] K. Kamada, Y. Furutani, Y. Sudo, N. Kamo, H. Kandori, Temperature-dependent interactions between photoactivated *pharaonis* phoborhodopsin and its transducer, Biochemistry 45 (2006) 4859–4866.
[114] C.S. Yang, J.L. Spudich, Light-induced structural changes occur in the transmembrane helices of the *Natronobacterium pharaonis* HtrII transducer, Biochemistry 40 (2001) 14207–14214.
[115] E.N. Spudich, W. Zhang, M. Alam, J.L. Spudich, Constitutive signaling by the phototaxis receptor sensory rhodopsin II from disruption of its protonated Schiff base-Asp-73 interhelical salt bridge, Proc. Natl. Acad. Sci. U. S. A. 94 (1997) 4960–4965.
[116] J. Sasaki, T. Nara, E.N. Spudich, J.L. Spudich, Constitutive activity in chimeras and deletions localize sensory rhodopsin II/HtrII signal relay to the membrane-inserted domain, Mol. Microbiol. 66 (2007) 1321–1330.
[117] M. Hein, I. Radu, J.P. Klare, M. Engelhard, F. Siebert, Consequences of counterion mutation in sensory rhodopsin II of *Natronobacterium pharaonis* for photoreaction and receptor activation: an FTIR study, Biochemistry 43 (2004) 995–1002.
[118] A.K. Sharma, J.L. Spudich, W.F. Doolittle, Microbial rhodopsins: functional versatility and genetic mobility, Trends Microbiol. 14 (2006) 463–469.
[119] K. Ihara, T. Umemura, I. Katagiri, T. Kitajima-Ihara, Y. Sugiyama, Y. Kimura, Y. Mukohata, Evolution of the archaeal rhodopsins: evolution rate changes by gene duplication and functional differentiation, J. Mol. Biol. 285 (1999) 163–174.
[120] G. Schmies, M. Engelhard, P.G. Wood, G. Nagel, E. Bamberg, Electrophysiological characterization of specific interactions between bacterial sensory rhodopsins and their transducers, Proc. Natl. Acad. Sci. U. S. A. 98 (2001) 1555–1559.
[121] T. Rink, M. Pfeiffer, D. Oesterhelt, K. Gerwert, H.J. Steinhoff, Unraveling photoexcited conformational changes of bacteriorhodopsin by time resolved electron paramagnetic resonance spectroscopy, Biophys. J. 78 (2000) 1519–1530.
[122] M. Kataoka, H. Kamikubo, Structures of photointermediates and their implications for the proton pump mechanism, Biochim. Biophys. Acta 1460 (2000) 166–176.
[123] H.W. Choe, Y.J. Kim, J.H. Park, T. Morizumi, E.F. Pai, N. Krauss, K.P. Hofmann, P. Scheerer, O.P. Ernst, Crystal structure of metarhodopsin II, Nature 471 (2011) 651–655.
[124] D.L. Farrens, C. Altenbach, K. Yang, W.L. Hubbell, H.G. Khorana, Requirement of rigid-body motion of transmembrane helices for light activation of rhodopsin, Science 274 (1996) 768–770.
[125] H. Bolhuis, P. Palm, A. Wende, M. Falb, M. Rampp, F. Rodriguez-Valera, F. Pfeiffer, D. Oesterhelt, The genome of the square archaeon *Haloquadratum walsbyi*: life at the limits of water activity, BMC Genomics 7 (2006) 169.
[126] K. Inoue, L. Reissig, M. Sakai, S. Kobayashi, M. Homma, M. Fujii, H. Kandori, Y. Sudo, Absorption spectra and photochemical reactions in a unique photoactive protein, middle rhodopsin MR, J. Phys. Chem. B 116 (2012) 5888–5899.
[127] Y. Furutani, T. Okitsu, L. Reissig, M. Mizuno, M. Homma, A. Wada, Y. Mizutani, Y. Sudo, Large Spectral Change due to Amide Modes of a beta-Sheet upon the Formation of an Early Photointermediate of Middle Rhodopsin, J. Phys. Chem. B 117 (2013) 3449–3458.
[128] T. Kitajima-Ihara, Y. Furutani, D. Suzuki, K. Ihara, H. Kandori, M. Homma, Y. Sudo, *Salinibacter* sensory rhodopsin: sensory rhodopsin I-like protein from a eubacterium, J. Biol. Chem. 283 (2008) 23533–23541.
[129] S.P. Balashov, J.K. Lanyi, Xanthorhodopsin: Proton pump with a carotenoid antenna, Cell. Mol. Life Sci. 64 (2007) 2323–2328.
[130] E.F. Mongodin, K.E. Nelson, S. Daugherty, R.T. Deboy, J. Wister, H. Khouri, J. Weidman, D.A. Walsh, R.T. Papke, G. Sanchez Perez, A.K. Sharma, C.L. Nesbo, D. MacLeod, E. Bapteste, W.F. Doolittle, R.L. Charlebois, B. Legault, F. Rodriguez-Valera, The genome of *Salinibacter ruber*: convergence and gene exchange among hyperhalophilic bacteria and archaea, Proc. Natl. Acad. Sci. U. S. A. 102 (2005) 18147–18152.
[131] D. Suzuki, Y. Furutani, K. Inoue, T. Kikukawa, M. Sakai, M. Fujii, H. Kandori, M. Homma, Y. Sudo, Effects of chloride ion binding on the photochemical properties of *salinibacter* sensory rhodopsin I, J. Mol. Biol. 392 (2009) 48–62.
[132] K. Inoue, Y. Sudo, M. Homma, H. Kandori, Spectrally silent intermediates during the photochemical reactions of *Salinibacter* sensory rhodopsin I, J. Phys. Chem. B 115 (2011) 4500–4508.
[133] R.A. Bogomolni, J.L. Spudich, The photochemical reactions of bacterial sensory rhodopsin-I. Flash photolysis study in the one microsecond to eight second time window, Biophys. J. 52 (1987) 1071–1075.
[134] Y. Furutani, H. Takahashi, J. Sasaki, Y. Sudo, J.L. Spudich, H. Kandori, Structural changes of sensory rhodopsin I and its transducer protein are dependent on the protonated state of Asp76, Biochemistry 47 (2008) 2875–2883.
[135] B. Schobert, J.K. Lanyi, D. Oesterhelt, Effects of anion binding on the deprotonation reactions of halorhodopsin, J. Biol. Chem. 261 (1986) 2690–2696.
[136] G. Váró, L.S. Brown, J. Sasaki, H. Kandori, A. Maeda, R. Needleman, J.K. Lanyi, Light-driven chloride ion transport by halorhodopsin from *Natronobacterium pharaonis*. 1. The photochemical cycle, Biochemistry 34 (1995) 14490–14499.
[137] H. Irieda, L. Reissig, A. Kawanabe, M. Homma, H. Kandori, Y. Sudo, Structural characteristics around the beta-ionone ring of the retinal chromophore in *Salinibacter* sensory rhodopsin I, Biochemistry 50 (2011) 4912–4922.
[138] D. Suzuki, Y. Sudo, Y. Furutani, H. Takahashi, M. Homma, H. Kandori, Structural changes of *Salinibacter* sensory rhodopsin I upon formation of the K and M photointermediates, Biochemistry 47 (2008) 12750–12759.
[139] L. Reissig, T. Iwata, T. Kikukawa, M. Demura, N. Kamo, H. Kandori, Y. Sudo, Influence of halide binding on the hydrogen bonding network in the active site of *Salinibacter* sensory rhodopsin I, Biochemistry 51 (2012) 8802–8813.
[140] J. Yagasaki, D. Suzuki, K. Ihara, K. Inoue, T. Kikukawa, M. Sakai, M. Fujii, M. Homma, H. Kandori, Y. Sudo, Spectroscopic studies of a sensory rhodopsin I homologue from the archaeon *Haloarcula vallismortis*, Biochemistry 49 (2010) 1183–1190.
[141] Y. Sudo, Y. Yuasa, J. Shibata, D. Suzuki, M. Homma, Spectral tuning in sensory rhodopsin I from *Salinibacter ruber*, J. Biol. Chem. 286 (2011) 11328–11336.
[142] Y. Sudo, A. Okada, D. Suzuki, K. Inoue, H. Irieda, M. Sakai, M. Fujii, Y. Furutani, H. Kandori, M. Homma, Characterization of a signaling complex composed of sensory rhodopsin I and its cognate transducer protein from the eubacterium *Salinibacter ruber*, Biochemistry 48 (2009) 10136–10145.
[143] M. Iwamoto, Y. Sudo, K. Shimono, N. Kamo, Selective reaction of hydroxylamine with chromophore during the photocycle of *pharaonis* phoborhodopsin, Biochim. Biophys. Acta 1514 (2001) 152–158.
[144] Y. Sudo, M. Iwamoto, K. Shimono, N. Kamo, Association of *pharaonis* phoborhodopsin with its cognate transducer decreases the photo-dependent reactivity by water-soluble reagents of azide and hydroxylamine, Biochim. Biophys. Acta 1558 (2002) 63–69.
[145] J. Vonck, Structure of the bacteriorhodopsin mutant F219L N intermediate revealed by electron crystallography, EMBO J. 19 (2000) 2152–2160.
[146] N. Radzwill, K. Gerwert, H.J. Steinhoff, Time-resolved detection of transient movement of helices F and G in doubly spin-labeled bacteriorhodopsin, Biophys. J. 80 (2001) 2856–2866.
[147] H. Yoshida, Y. Sudo, K. Shimono, M. Iwamoto, N. Kamo, Transient movement of helix F revealed by photo-induced inactivation by reaction of a bulky SH-reagent to cysteine-introduced *pharaonis* phoborhodopsin (sensory rhodopsin II), Photochem. Photobiol. Sci. 3 (2004) 537–542.
[148] O.A. Sineshchekov, J. Sasaki, B.J. Phillips, J.L. Spudich, A Schiff base connectivity switch in sensory rhodopsin signaling, Proc. Natl. Acad. Sci. U. S. A. 105 (2008) 16159–16164.
[149] J.A. Bornhorst, J.J. Falke, Quantitative analysis of aspartate receptor signaling complex reveals that the homogeneous two-state model is inadequate: development of a heterogeneous two-state model, J. Mol. Biol. 326 (2003) 1597–1614.
[150] S. Asakura, H. Honda, Two-state model for bacterial chemoreceptor proteins. The role of multiple methylation, J. Mol. Biol. 176 (1984) 349–367.
[151] S.H. Kim, W. Wang, K.K. Kim, Dynamic and clustering model of bacterial chemotaxis receptors: structural basis for signaling and high sensitivity, Proc. Natl. Acad. Sci. U. S. A. 99 (2002) 11611–11615.
[152] K.H. Jung, V.D. Trivedi, J.L. Spudich, Demonstration of a sensory rhodopsin in eubacteria, Mol. Microbiol. 47 (2003) 1513–1522.
[153] L. Vogeley, O.A. Sineshchekov, V.D. Trivedi, J. Sasaki, J.L. Spudich, H. Luecke, *Anabaena* sensory rhodopsin: a photochromic color sensor at 2.0 A, Science 306 (2004) 1390–1393.
[154] O.A. Sineshchekov, E.N. Spudich, V.D. Trivedi, J.L. Spudich, Role of the cytoplasmic domain in *Anabaena* sensory rhodopsin photocycling: vectoriality of Schiff base deprotonation, Biophys. J. 91 (2006) 4519–4527.
[155] L. Shi, S.R. Yoon, A.G. Bezerra Jr., K.-H. Jung, L.S. Brown, Cytoplasmic shuttling of protons in *anabaena* sensory rhodopsin: implications for signaling mechanism, J. Mol. Biol. 358 (2006) 686–700.

[156] A. Kawanabe, Y. Furutani, K.H. Jung, H. Kandori, Photochromism of *Anabaena* sensory rhodopsin, J. Am. Chem. Soc. 129 (2007) 8644–8649.
[157] L. Vogeley, V.D. Trivedi, O.A. Sineshchekov, E.N. Spudich, J.L. Spudich, H. Luecke, Crystal structure of the *Anabaena* sensory rhodopsin transducer, J. Mol. Biol. 367 (2007) 741–751.
[158] X. Chen, J.L. Spudich, Demonstration of 2:2 stoichiometry in the functional SRI-HtrI signaling complex in *Halobacterium* membranes by gene fusion analysis, Biochemistry 41 (2002) 3891–3896.
[159] J.L. Spudich, The multitalented microbial sensory rhodopsins, Trends Microbiol. 14 (2006) 480–487.
[160] D.M. Kehoe, Chromatic adaptation and the evolution of light color sensing in cyanobacteria, Proc. Natl. Acad. Sci. U. S. A. 107 (2010) 9029–9030.
[161] H. Irieda, T. Morita, K. Maki, M. Homma, H. Aiba, Y. Sudo, Photo-induced regulation of the chromatic adaptive gene expression by *Anabaena* sensory rhodopsin, J. Biol. Chem. 287 (2012) 32485–32493.
[162] S. Wang, R.A. Munro, S.Y. Kim, K.H. Jung, L.S. Brown, V. Ladizhansky, Paramagnetic relaxation enhancement reveals oligomerization interface of a membrane protein, J. Am. Chem. Soc. 134 (2012) 16995–16998.
[163] T. Sasaki, M. Kubo, T. Kikukawa, M. Kamiya, T. Aizawa, K. Kawano, N. Kamo, M. Demura, Halorhodopsin from *Natronobacterium pharaonis* forms a trimer even in the presence of a detergent, dodecyl-beta-D-maltoside, Photochem. Photobiol. 85 (2009) 130–136.
[164] Y. Yamashita, T. Kikukawa, T. Tsukamoto, M. Kamiya, T. Aizawa, K. Kawano, S. Miyauchi, N. Kamo, M. Demura, Expression of *salinarum* halorhodopsin in *Escherichia coli* cells: solubilization in the presence of retinal yields the natural state, Biochim. Biophys. Acta 1808 (2011) 2905–2912.
[165] T. Tsukamoto, T. Sasaki, K.J. Fujimoto, T. Kikukawa, M. Kamiya, T. Aizawa, K. Kawano, N. Kamo, M. Demura, Homotrimer formation and dissociation of *pharaonis* halorhodopsin in detergent system, Biophys. J. 102 (2012) 2906–2915.
[166] T. Tsukamoto, T. Kikukawa, T. Kurata, K.H. Jung, N. Kamo, M. Demura, Salt bridge in the conserved His-Asp cluster in *Gloeobacter* rhodopsin contributes to trimer formation, FEBS Lett. 587 (2013) 322–327.
[167] L. Essen, R. Siegert, W.D. Lehmann, D. Oesterhelt, Lipid patches in membrane protein oligomers: crystal structure of the bacteriorhodopsin-lipid complex, Proc. Natl. Acad. Sci. U. S. A. 95 (1998) 11673–11678.